https://doi.org/10.5194/essd-2025-723
Preprint. Discussion started: 4 March 2026

Open Access Earth System Science Data Discussions

EMO-1: an improved version of the high-resolution multi-variable gridded meteorological dataset for Europe

Peter Salamon[1], Tim Sperzel[2], Goncalo Gomes[3], Marco Radke-Fretz[4], Carina-Denise Lemke[8], Carlo Russo[5], Christoph Schweim[4], Ervin Zsoter[7], Alessandro Dosio[1], Mariapina Vomero[6], Markus Ziese[2], Stefania Grimaldi[1]

[1] European Commission - Joint Research Centre, Ispra, Italy
[2] Deutscher Wetterdienst, Offenbach am Main, Germany
[3] WTP (Westpole Italy), Milan, Italy
[4] KISTERS AG, Aachen, Germany
[5] UniSystems, Milan, Italy
[6] Institute for Marine and Antarctic Studies, University of Tasmania, Hobart, Tasmania, Australia
[7] European Center for Medium-Range Weather Forecasts, Reading, UK
[8] City of Regensburg, Regensburg, Germany

Correspondence to: Peter Salamon (peter.salamon@ec.europa.eu)

Abstract.

High-quality, gridded meteorological datasets are essential for continental-scale hydrological modelling. This paper introduces EMO-1, an advanced version of the European Meteorological Observations (EMO) dataset, developed to support the operational European Flood Awareness System (EFAS) of the Copernicus Emergency Management Service. EMO-1 provides daily and 6-hourly meteorological fields across Europe at a high spatial resolution of 1 arc-minute (~1.5 km) covering the period from 1990 to 2024. The dataset represents a substantial upgrade over its predecessor, EMO-5, integrating observations from 47 data providers and increasing significantly the number of stations used for interpolation. It harmonizes heterogeneous data from in-situ stations and integrates "virtual stations" from high-resolution regional grids and ERA5-Land to minimize data gaps in regions with very low station density. The dataset covers eight variables: daily and 6-hourly total precipitation, minimum and maximum air temperature, 6-hourly average air temperature, daily mean wind speed, solar radiation, and water vapor pressure. A rigorous, two-tier quality control system is applied to filter erroneous observations before processing. For interpolation EMO-1 uses an open-source implementation of the Angular Distance Weighting (ADW) scheme. Cross-validation results demonstrate that ADW maintains interpolation skill comparable to other deterministic methods while offering superior computational efficiency and reproducibility. EMO-1 prioritizes station density and timeliness to serve operational forecasting needs, although the resulting spatial-temporal heterogeneity makes it less suitable for long-term trend analysis. The dataset is openly available under a Creative Commons Attribution 4.0 license via the Joint Research Centre Data Catalogue, with foreseen annual updates and accessible open-source interpolation software to foster transparency and community collaboration.

https://doi.org/10.5194/essd-2025-723
Preprint. Discussion started: 4 March 2026

Open Access Earth System Science Data Discussions

1 Introduction

Observation-based, gridded meteorological datasets have a wide range of applications from supporting hydrological modelling (e.g. Hundecha et al., 2020), evaluating and, eventually, post-processing climate model outputs (e.g. Dosio, 2016; Dosio et al., 2021; Vautard et al., 2021) or increasing our confidence in the attribution of past climate changes and, ultimately, in future climate projections (e.g. Doblas-Reyes et al., 2021). Gridded meteorological datasets at continental (e.g., Cornes et al., 2018) or even global scales (e.g. Adler et al., 2018, Contractor et al., 2020) enable the analysis of large-scale climate patterns (e.g. Copernicus Climate Change Service and World Meteorological Organization, 2025) and the development of continental and global modelling and forecasting activities (e.g., Matthews et al., 2024; World Meteorological Organization, 2024) supporting policy and decision making at European and global level. However, to create such valuable datasets requires a significant effort for the collection, harmonization, quality checking, and processing of station data. For example, in Europe, station-based meteorological observations are typically collected by national hydrometeorological authorities and regional or local environmental and water basin authorities. The European Meteorological Observations (EMO)-5 dataset, presented by Thiemig et al. (2022), had included data from 24 different data providers. Most of these data providers deliver the data in different formats with different metadata, through varying access points and with diverse license conditions resulting in a significant effort to create such large-scale gridded datasets.

As described by Thiemig et al. (2022), the EMO dataset is collected as part of the Copernicus Emergency Management Service and with the aim to support the European Flood Awareness System (EFAS - Matthews et al., 2024). EFAS depends heavily on quality-controlled, (sub-) daily meteorological information on precipitation, air temperature, wind speed, solar radiation, and water vapour pressure for (a) hydrological model calibration and validation as well as for (b) the computation of initial conditions for the hydrological model during the operational running. Thus, EMO prioritizes station density at each time step, in particular for the near-real time data collection, in contrast to datasets such as E-OBS (Cornes et al., 2018) that aim at emphasizing station homogeneity.

In this paper we present EMO-1, an improved version of the EMO-5 dataset (Thiemig et al., 2022) which includes the following main changes: (1) increase in the number of meteorological observations used; (2) increase in spatial resolution of the meteorological grids from 5 km to 1 arc minute (approx. 1.5 km), model domain, and change in the geographical projection of the grids to WGS 84; (3) increase in the temporal coverage of the dataset from 1990 until 2024 with a foreseen regular annual update; and (4) change in the interpolation method from SPHEREMAP (Becker et al., 2013, Willmott et al., 1985) to an open-source implementation of the angular distance weighting scheme (Shepard, 1968).

The remainder of this paper is organized as follows: The source data are described in Sect. 2. The entire workflow from quality control to the interpolation of grids is described in Sect. 3. Data access information is given in Sect. 4. Finally, conclusions are presented in Sect. 5, followed by an outlook.

https://doi.org/10.5194/essd-2025-723
Preprint. Discussion started: 4 March 2026

2 Input data

EMO-1 uses data from 47 data providers (i.e. 41 station data providers plus 6 gridded dataset providers) which represents a 95% increase in comparison to EMO-5. Most data providers are national meteorological services but there are also regional environmental and river basin authorities and some international data providers. The full list of all data providers contributing to EMO-1 is described in Appendix A, Table 5.

Surface observations that are collected and used for gridding include precipitation, air temperature, 10 m wind speed, solar radiation, and water vapour pressure (Table 1). In addition, 10 m wind direction, cloud cover, sunshine duration, relative air humidity, evaporation, and dew point temperature are collected but currently not used for gridding. As EMO-1 is used to support the operational EFAS, surface observations are collected in near real-time as well as for historic periods. It should be noted that data are provided with various temporal resolutions and aggregation intervals, depending on the parameter and data provider. The highest received temporal resolution and accumulation period is one minute (air temperature and precipitation from one data provider). Instantaneous parameters, like air temperature or wind speed, are mainly provided with temporal resolution of one, three, and six hours, but also with higher and lower temporal resolutions. Most provided precipitation totals are accumulated over six and twelve hours, but also daily and one hourly totals are often provided. Minimum and maximum air temperature are mostly provided with daily aggregation. More details about the aggregation and post-processing of the received meteorological observations to the required time periods as indicated in Table 1 are described in section 3.2.

Table 1 Definition of meteorological variables as used in EMO-1

Parameter	Period	Abbreviation	Unit	Description
total precipitation	daily	pr	mm/day	total precipitation between 6 UTC on the day specified and 6 UTC on the previous day
total precipitation	6-hourly	pr6	mm/6h	total precipitation
minimum air temperature	daily	tn	°C	minimum air temperature between 18 UTC and 6 UTC (i.e. during the preceding night) at 2 m
maximum air temperature	daily	tx	°C	maximum air temperature between 6 UTC and 18 UTC (i.e. during daytime) at 2m
average air temperature	6-hourly	ta6	°C	Average air temperature at 2m
average wind speed	daily	ws	m/s	mean wind speed at 10 metres (0-24 UTC)
solar radiation	daily	rg	J/m^2	accumulated downward surface solar radiation (0-24 UTC)
water vapour pressure	daily	pd	hPa	mean water vapour pressure (0-24 UTC)

https://doi.org/10.5194/essd-2025-723
Preprint. Discussion started: 4 March 2026

Like EMO-5, EMO-1 integrates also information from gridded datasets for specific time periods with the aim to cover areas with very low station density or to improve the quality over pronounced orography (see Thiemig et al., 2022). Information from the gridded datasets is mostly used for the variable precipitation (see Appendix A, Table 6). Each selected grid point is treated as a virtual station. However, to ensure computational efficiency only a subset of grid points is used and therefore the gridded datasets are not used in their original resolution. For the four high-resolution regional gridded datasets a regular subset of grid points with horizontal resolution of around 10×10 km was chosen whereas for ERA-5 Land (Hersbach et al., 2023) a subset with a spacing of 0.5° was selected. Virtual stations from ERA-5 Land were only used in the low station density areas in the East, South, and North-West area of the spatial domain (see Figure 3). To ensure that in those areas real station observation, when available, are given higher preference above the virtual stations from ERA-5 Land a specific protocol was introduced during the gridding procedure which is described in section 3.3. It is important to note that from March 2022 onwards meteorological data from a large portion of Ukrainian weather stations have not been available anymore or reported only sporadically. As this can lead to a significant degradation of the quality of the meteorological fields as an exceptional measure, the gridded data from the numerical weather prediction model ICON from the German Weather Service has been integrated for Ukraine. This includes the variables precipitation (daily and 6-hourly) as well as wind speed. Like the ERA-5 Land gridded data, the selected grid points are treated as virtual stations. The main characteristics of the 6 input meteorological data grids underlying EMO-1 are summarized in Appendix A.

2.1 Quality control of input data

Although the station data is usually quality controlled by the data providers, a series of quality control procedures has been applied based on the experience that both real-time and historical data may still contain erroneous measurements occasionally. The quality control procedures are applied in three stages: (1) synchronous data validation which is applied automatically when station data is imported into the database; (2) asynchronous data validation which is triggered manually; and (3) final visual checks to exclude manually any data values not identified by the previous checks. If any of the quality control procedures fails for a specific observation the value is flagged and excluded from gridding.

Synchronous Data Validation entails three principles: (1) the comparison between imported values and lower/upper threshold values; (2) the cross-validation with related variables (where relevant related variables are available); (3) rate of change of the registered values (only applied to air temperature). For the comparison between imported values and lower/upper threshold values, geographically and seasonally varying thresholds have been derived for the variables air temperature, solar radiation, and vapour pressure. To define appropriate lower and upper threshold values for different seasons and geographical (climate-derived) zones, several percentiles were calculated using all meteorological station observations between 1990 and 2021 within each climate zone in the database. The geographical (climate) zones are based on the Köppen-Geiger climate classification (Kottek et al., 2006). For the lower limit, the 0.01%, 0.1%, 1%, and 5% percentiles were calculated. The 95%, 99%, 99.9%, and 99.99% percentiles were computed to assess possible upper limits. The distribution curves were smoothed by a seven-day low-pass filter. The percentiles for each meteorological variable and climate zone were visually checked to define the upper

https://doi.org/10.5194/essd-2025-723
Preprint. Discussion started: 4 March 2026

and lower thresholds for the comparison including a buffer which is based on expert judgement. This buffer aims to reduce the risk of eliminating real observations connected to extreme (not yet observed) meteorological events. An example of the percentiles for air temperature in the climate zone Cfb (warm temperate climate, fully humid, warm summer) and the selected upper and lower thresholds including the expert-based buffer is shown in Figure 1. For some variables and climate zones, adequate statistical analysis was not possible due to the low number of observations. In such cases, the data validation protocol uses fixed upper and lower threshold values as reported in Table 2. Finally, wind speed makes use of upper and lower threshold values which are constant in space and time as the historical values of this variable did not show any dependency on season or climate zone (see also Table 2).

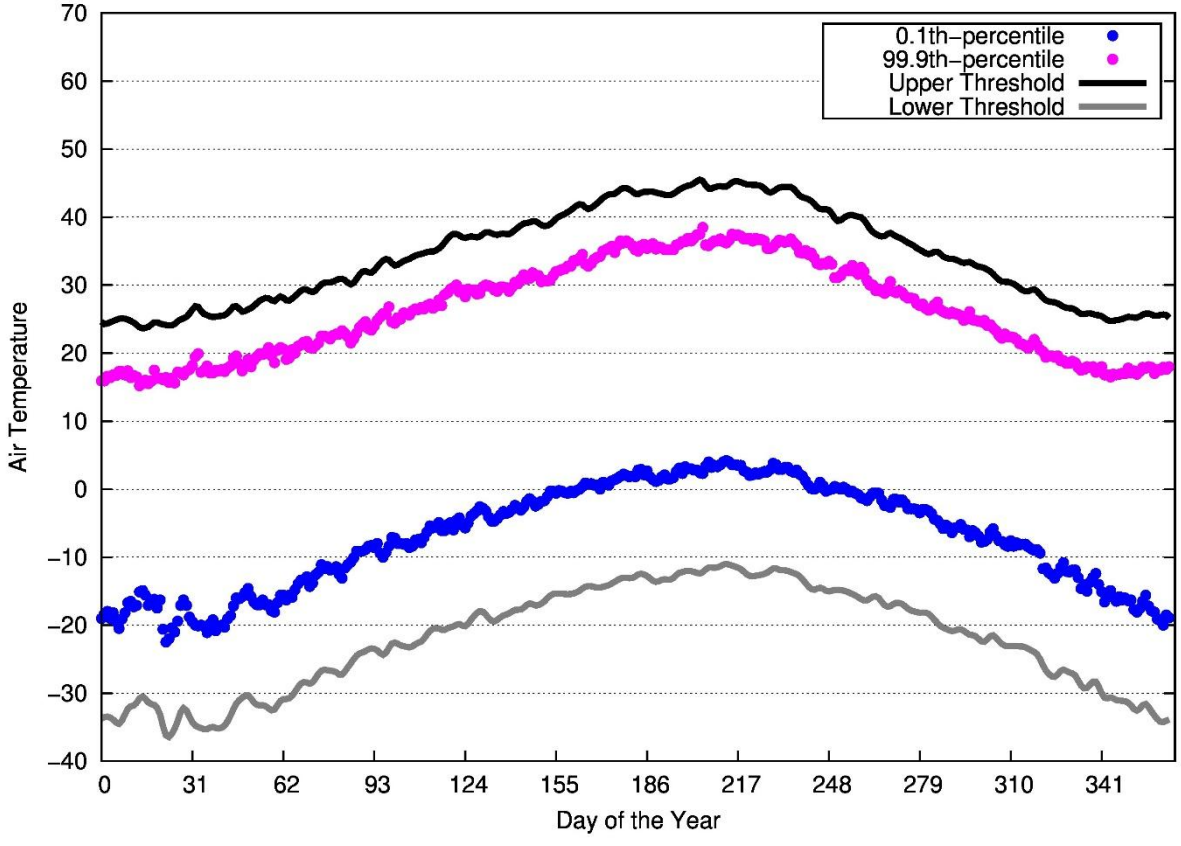

Figure 1 Percentiles and selected upper/lower thresholds for the synchronous data validation checks for air temperature in climate zone Cfb

https://doi.org/10.5194/essd-2025-723
Preprint. Discussion started: 4 March 2026

Similarly, thresholds for precipitation do not depend on season or climate zone. Different threshold values are used for different aggregation periods based on historic records of precipitation and on expert judgment (see Table 3).

Table 2 Fixed upper and lower thresholds for comparison for variables not showing a dependency on season and climate or where the number of observations were too low for a statistical analysis

Meteorological variable	Minimum threshold	Maximum threshold
wind speed	0 m/s	50 m/s
solar radiation	0	1360 cos(lat) W/m^2
water vapour pressure	0 hPa	35 hPa

Table 3 Thresholds for precipitation depending on the aggregation interval

Aggregation interval [mins]	Maximum precipitation threshold [mm]
15	125
30	200
60	250
180	350
360	425
540	475
720	500
900	525
1080	550
1440	600

The cross-validation of values against data from related parameters at the same station is carried out for dew point temperature against air temperature (dew point temperature should be lower than air temperature, note that dew point temperature is collected but not used for gridding in EMO-1) and for wind speed against wind direction (both must either indicate the presence of wind, i.e. non-zero values, or the absence of wind; wind direction is collected but not used for gridding in EMO-1). Rate of change validation is applied only to air temperature with the thresholds depending on the observation interval. For example, the maximum allowed variations are 15 degrees and 30 degrees if data are delivered with hourly and daily frequency, respectively.

The asynchronous data validation quality control procedures applied to the input data of EMO-1 contains rules on flatliner detection, aggregation comparison (e.g. sum of four 6-hourly precipitation should be nearly identical to the daily precipitation for the same time period), detection of inconsistent observations from spatial duplicates (spatial duplicates-rule identifies stations for which data are delivered by different data providers) and spatial (zero) comparison.

Flatliner detection has been applied to precipitation, wind speed, and air temperature. For precipitation, the rule is intended to detect unusually long periods of 0.0 mm precipitation and remove them from further processing. For this purpose, the most

https://doi.org/10.5194/essd-2025-723
Preprint. Discussion started: 4 March 2026

frequently occurring climate zones in the model domain were grouped into "fully humid" and "summer dry", whereby a distinction is also made between summer months (AMJJAS) and winter months (ONDJFM) for the case of stations in summer dry climate zones. Several stations from the respective climate zones were randomly examined in order to identify realistic dry periods as limit values. This resulted in a limit value of max. 91 days without precipitation for stations in the "fully humid" and "summer dry"-winter group, and max. 151 days for the "summer dry"-summer group.

For wind speed, the flatliner rule was implemented to filter out equal, consecutive values. If the station reports the same wind speed for longer than 48 hours, it is assumed that the sensor is defective, and these values are excluded from further processing. The 48 hours limit is used in time series with time resolutions higher than daily. If only one value is supplied per day, the limit is 4 consecutive days with the same value. The temporal thresholds were the outcome of expert judgement. Like wind speed, for air temperature the aim is to mark consecutive identical values, as this is likely to indicate a sensor error. For the sub-daily temporal resolutions, the limit is set to 48 hours whereas for the daily minimum and maximum temperatures a limit of 8 consecutive days with the same value is applied.

The aggregation comparison rule was only applied for the variable precipitation and was configured to check time series of the same parameter provided by the same station. If a station reports the same parameter in several time aggregations (e.g. hourly, 6-hourly, daily), the values aggregated to higher time intervals must be consistent with the values reported in the higher time aggregations. For example, the sum of four 6-hour precipitation values must be nearly identical as the daily reported precipitation value (a small discrepancy due to rounding of the observed values is tolerated).

EMO-1 includes observations from stations that have been reported from different data providers (e.g. stations reported via the SYNOP network are often also included in the stations received by a national or regional data provider). Values for the same station and the same time step should be the same, regardless of the data provider. However, in practice, these values are not necessarily always identical due to different methods of data processing and transfer applied by different data providers. The spatial-duplicates rule identifies stations for the variable precipitation for which data are delivered by different data providers. If duplicate stations have different values for a given time stamp (note that small discrepancies that could be due to rounding or other reasons are tolerated), the values for this corresponding time stamp are flagged as “rejected” and excluded from further processing. Station coordinates given by different data providers for the same station are not always identical; therefore, duplicates are identified by selecting stations which have a maximum distance of 1.5 km.

Finally, the spatial and spatial-zero comparison rules check time series data of the variable precipitation at the target station against a range of values from neighbouring stations. The spatial (zero) comparison rule looks for up to eight neighbouring stations within a search radius of 50 km and a priority radius of 30 km (the search radiuses were retrieved from the analysis of precipitation station density in the model domain), and a maximum elevation difference of 200 m. It then selects the closest stations from each of the four cardinal directions. If less than 3 neighbouring stations can be identified, the rule is not applied. The spatial zero comparison rule then rejects 0.0 mm values from a station if all neighbouring stations have recorded at least 5.0 mm or more precipitation whereas the spatial comparison rule rejects values which are out of the confidence interval of the selected neighbouring stations. The confidence intervals for the spatial comparison rule account for the mean and standard

https://doi.org/10.5194/essd-2025-723
Preprint. Discussion started: 4 March 2026

deviation of the values recorded at the neighbouring stations, multiplied by ad-hoc factors, with the aim to identify and remove unrealistically high precipitation values which can produce significant issues when used for hydrological modeling in particular. More details about the spatial comparison rule can be found in Lemke et al. (2023).

3 Methodology

3.1 Post-processing of station data

In case the meteorological observations are not already provided in the correct temporal resolution as outlined in Table 1, the observations are post-processed to calculate the daily and 6-hourly (precipitation and temperature only) mean / minimum / maximum / sums.

Aggregation of the different variables has been performed in accordance with the WMO Guidelines (World Meteorological Organization, 2019). Daily precipitation totals must be provided as aggregated values from 6 UTC to 6 UTC of the following day. The minimum air temperature is the lowest temperature between 18 UTC and 6 UTC of the next day, whereas the maximum temperature is calculated from the observations taken between 6 UTC and 18 UTC. For precipitation, the 12-hourly and 6-hourly totals have been disaggregated where necessary to derive the missing 6-hourly total.

To aggregate station observations from higher temporal resolutions to 6-hourly and daily resolutions, as required by EMO-1, a minimum level of data coverage is necessary to accurately compute minimum, maximum, and mean values, as well as aggregated totals. Precipitation totals are only computed if the aggregation period is fully covered by observational data (coverage = 100%). For all other parameters, a coverage of 87% is required. An exception is made for six and twelve hourly means with a minimum coverage of 66% to consider stations reporting with a temporal resolution of six hours.

Given that precipitation is the most important variable for rainfall-runoff modeling and provided that the operational EFAS (Matthews et al., 2024) requires 6-hourly inputs, daily precipitation values for some data providers (see Appendix A) have been decumulated to ensure a reasonable coverage of precipitation observations in areas with a particularly low station density. The decumulation algorithm first checks if a corresponding 6-hourly observation for the same station already exists or is available from another station within a radius of 1.5 km. If this is not the case, it decumulates the daily value either into 4 equal 6-hourly values or, where partial 6-hourly observations exist, it decumulates the daily value considering the partial 6-hourly observations. Note that this disaggregation method can potentially introduce inhomogeneities and might impact the statistical properties of the extreme statistics of the 6-hour values, particularly where daily values are split into 4 equal 6-hourly values. More sophisticated methods, with better statistical behaviour, will be explored in future versions of the data set.

3.2 Interpolation method

Several interpolation algorithms for meteorological variables have been proposed in literature, and these algorithms can be broadly classified in deterministic methods and geostatistical models. Deterministic methods assume that the interpolated surfaces are more influenced by nearby points and less by distant points. The values at interpolation points depend on

https://doi.org/10.5194/essd-2025-723
Preprint. Discussion started: 4 March 2026

mathematical formulas that control the smoothness of the interpolated surface. Geostatistical methods include statistical relationships between the sample points (i.e., autocorrelation).

The studies reported in literature demonstrated that there is no interpolation method that stands out as superior to others. Conversely, several methods perform best for different station densities, variables, climate regimes, geographical domain, and evaluation criteria. The main control on interpolation skill is the density of the station network, with topographic complexity, climatological features, and seasonality as compounding factors (Camera et al., 2014; Hofstra et al., 2008; Thiemig et al., 2022; Yang & Xing, 2021). Hence, tailored analysis is necessary to determine the most indicated interpolation method for each application. With reference to relevant examples of applications at the European to global scale, Hofstra et al. (2008) and Schamm et al.(2014) selected a geostatistical approach; Becker et al.(2013) and Thiemig et al.(2022) selected a deterministic approach.

Albeit of primary importance, interpolation accuracy is not the only factor in the selection of the most suitable algorithm for large scale implementations, especially in the framework of operational systems such as EFAS as is the case for EMO-1. Other relevant selection criteria are computational cost, robustness, accessibility, maintainability, and numerical stability of the implemented algorithm. The selection of the interpolation algorithm for the generation of EMO-1 was driven by the following criteria:

- Adequate interpolation skill with precipitation as primary variable (this variable has the largest impact on the modelling of rainfall-runoff-routing processes).
- Fitness for operational use, i.e. stable, easy to maintain, and with fast execution times for near-real time applications.
- Computational efficiency

Unfortunately, the Spheremap algorithm (Becker et al., 2013) which has been used for EMO-5, and which has demonstrated a good performance in terms of error measures for the interpolation scheme (see Thiemig et al., 2022) has been implemented in a software which is not available as open-source. This limits not only the maintenance of the software but also the improvement of computational efficiency which was necessary due to the increase in the number of observations available for interpolation and the higher spatial resolution of the grids. For EMO-1, an open-source interpolation software, pyg2p (GitHub, https://github.com/ec-jrc/pyg2p), was developed and three deterministic methodologies were implemented and tested against Spheremap: 1.) Inverse Distance Weighting (IDW); 2.) Angular Distance Weighting (ADW) (Shepard, 1968); and 3.) Angular Distance Weighting with Correlation Decay Distance (CDD) (Hofstra & New, 2009). Geostatistical approaches, such as kriging, were discarded as they typically require automatic fitting of a variogram, which can represent a concern related to robustness and stability in an operational environment (Thiemig et al., 2022). To easily handle the parsing of input files containing the observations, choosing the desired interpolation method and producing the output in various formats an additional wrapper for pyg2p was used (gridding, https://github.com/ec-jrc/lisflood-utilities?tab=readme-ov-file#gridding).

IDW is the simplest algorithm as it only considers the geometrical distance between interpolation points and observations. Observations located closer to the target point have more influence (weight). ADW was conceived as an improvement to the original IDW as it includes information on direction and not only distance in the computation of the weights. Differently from

https://doi.org/10.5194/essd-2025-723
Preprint. Discussion started: 4 March 2026

Shepard (1968), the ADW implementation in pyg2p does not include slope or barrier information at interpolated data points to ensure that the exact observational value at each station is preserved during the interpolation which is important for variables such as precipitation. Finally, a variant of ADW uses the concept of CDD, also called correlation length scale or decorrelation length, to select the stations to be used in the interpolation and to compute the inverse-distance component of the station weight. CDD is defined as the distance where the correlation between one station and all other stations decays below 1/e (~0.36). A more detailed explanation of the three interpolation algorithms assessed here is provided in Shepard (1968) and Hofstra & New (2009).

We assessed the three interpolation methods applying the repeated stratified k-fold cross validation method (Pedregosa et al., 2011; Roberts et al., 2017) and benchmarked the results with Spheremap using the classic skill scores mean error (ME), mean square error (MSE), mean absolute error (MAE), Pearson correlation coefficient (R) and Critical Success Index (CSI). As we put more emphasis on the interpolation of 6-hourly precipitation values, we selected 56 dates with four 6-hourly steps for each date within the timespan 1990 – 2021 which included significant precipitation events in different geographical areas of the pan-European domain. Due to the large changes in the station density, the results for 6-hourly precipitation were computed (i) considering only the dates before 2008 and (ii) considering only the dates after 2010. It is here noted that the latter configuration of the stations network is the most similar to the configuration of the stations network used for the generation of the near-real-time gridded data.

Differently from ADW and IDW, Spheremap and CDD are not exact interpolators, meaning that both methods are not expected to exactly reproduce the values at the observation points. Hofstra & New (2009) noted that, for CDD, cross validation against station data does not allow a fair comparison. However, they expected the relative scores for cross validation to correspond to the relative skill of the interpolation method in estimating area average values at high spatial resolution.

Table 4 Summary of error measures for the selected interpolation schemes for 6-hourly total precipitation for dates before 2008 (left) and after 2010 (right). Best values are highlighted in bold.

	Spheremap		**IDW**		**ADW**		**CDD**	
	1990 - 2008	2010 – 2021	1990- 2008	2010 – 2021	1990 - 2008	2010 – 2021	1990 - 2008	2010 – 2021
MAE (mm)	0.935	1.039	0.997	1.015	0.940	**1.003**	**0.906**	1.372
MSE (mm^2)	4.658	7.879	4.625	**7.761**	4.745	7.920	**4.125**	8.970
ME (mm)	0.103	0.170	0.195	0.293	**0.098**	**0.147**	0.131	0.347
R (-)	0.835	0.894	0.832	**0.896**	0.833	0.895	**0.849**	0.875
CSI (-)	**0.853**	0.821	0.840	0.816	0.852	**0.823**	0.850	0.785

Table 4 shows the results for 6-hourly precipitation which is the most important variable for the operational EFAS. It can be seen that the performance of the four interpolation algorithms in terms of the different error measures is very similar which is

https://doi.org/10.5194/essd-2025-723
Preprint. Discussion started: 4 March 2026

in accordance with other studies (e.g. Hofstra & New, 2009). However, the scheme leading to the best values is different depending on the set of dates. ADW illustrates a slightly better performance than all other algorithms for the test cases from 2010 – 2021. CDD interpolation scheme has overall the highest performances for dates before 31.12.2008, which is when gridded datasets are more prominent (see Fig 2). When virtual and physical stations deliver different information, the interpolation scheme must accommodate different values in confining grid cells. The CDD scheme smoothing capability leads to the best results. ADW, being an exact interpolator, has overall slightly lower performances than CDD and Spheremap in the old years. Further results of the comparison of the algorithms for different precipitation thresholds and other meteorological variables (shown in Appendix B) indicate as well similar performance of the different interpolation algorithms. Therefore, due to its computational efficiency and its simplicity, EMO-1 uses ADW for the interpolation of the meteorological variables.

3.3 Grid creation

The model domain for which the meteorological grids are produced covers the European continent, extending further south into Northern Africa, parts of the Arabian Peninsula and middle East (Figure 3). The 1-arc minute domain uses WGS 84 longitude/latitude coordinates and sets the boundaries at: longitude 25.25°W - 50.25°E, latitude 22.75°N - 72.25°N. It is important to note that to avoid problems with gridding along the borders of the domain, station data is collected from a slightly larger region of -29.25°W - 54.25°E, 20.75°N - 74.25°N. A land–sea mask is used to exclude sea surfaces from the gridding procedure. Time stamps for the grids refer always to the end of the time interval.

For the variables temperature (min/max/mean) as well as for vapour pressure an orographic correction was applied to the station values before interpolation. We used altitude information from an upscaled version of the MERIT DEM (Yamazaki et al., 2017) as described in Choulga et al. (2024) to apply an adiabatic change of 0.006 Kelvin per height meter for temperature and 0.00025 hPa per height meter for water vapour pressure. Once the orographic correction was applied, the values were interpolated and brought back to the mean elevation of the respective grid cell by taking the parameter-specific correction factors into account.

All station observations (including the virtual stations from the gridded input datasets) that have passed the quality controls as described in Section 2.1 and that have been aggregated, where needed, to the required temporal resolution (6-hourly/daily) as indicated in Section 3.1 are used for interpolation. A special protocol is applied for daily and 6-hourly precipitation. As described in Section 2, in areas with very low station density ERA-5 Land was integrated by adding a subset of virtual stations with a spacing of 0.5° in the East, South, and North-West area of the spatial domain. However, while those areas have in general a low density of meteorological station observations, there are sometimes observations available for a specific variable and time-step. To ensure that higher preference is given to meteorological station observations a filter was implemented for the ERA-5 Land virtual stations removing the virtual stations in a radius of 100 km when an observation was available.

Figure 2 shows the number of stations used for interpolation in the period 1990 until 2024 for the different variables. As can be observed, the variables precipitation (6-hourly/daily) as well as air temperature (min/max/average) and wind speed have a comparably high number of observations, whereas solar radiation and vapour pressure use overall lower numbers of

https://doi.org/10.5194/essd-2025-723
Preprint. Discussion started: 4 March 2026

observations for the interpolation. All variables demonstrate a two- to threefold increase in number of available observations for gridding from 1990 until 2024. This is not unusual as more data from different data provider become available gradually for the more recent periods as is illustrated in Figure 4 which shows the availability of in-situ observations and gridded datasets for 6-hourly precipitation from the different data providers. For precipitation (6-hourly/daily) the total number of observations used for interpolation is strongly influenced by the availability of virtual stations from the regional gridded products and ERA-5 Land for the period 1990 until 2008 (see Figure 2a). As stated in section 2 this was done to compensate for low station density which can have a significant impact on the precipitation distribution in the dataset. Overall, when comparing the number of observations used in EMO-5 all variables in EMO-1 illustrate a significantly higher number of observations used for the interpolation.

For each of the meteorological variables, the location (and hence density) of the input data as well as the record length per station is shown in Figure 3. As can be expected, the number of stations for each variable are not regularly distributed. In general, higher station densities are observed in central and western Europe whereas the station density tends to be lower in southern and eastern Europe as well as northern Africa. As noted previously, the temporally and spatially inhomogeneous availability of stations leads to an inhomogeneous time series of grid-cell values, and therefore the EMO-1 dataset is not optimized for trend (or temporal) analyses. High-resolution figures representing the location of the input data as shown in Figure 3 and the availability in time as shown in Figure 4 for all meteorological variables can be found in Appendix A.

https://doi.org/10.5194/essd-2025-723
Preprint. Discussion started: 4 March 2026

Open Access Earth System Science Data Discussions

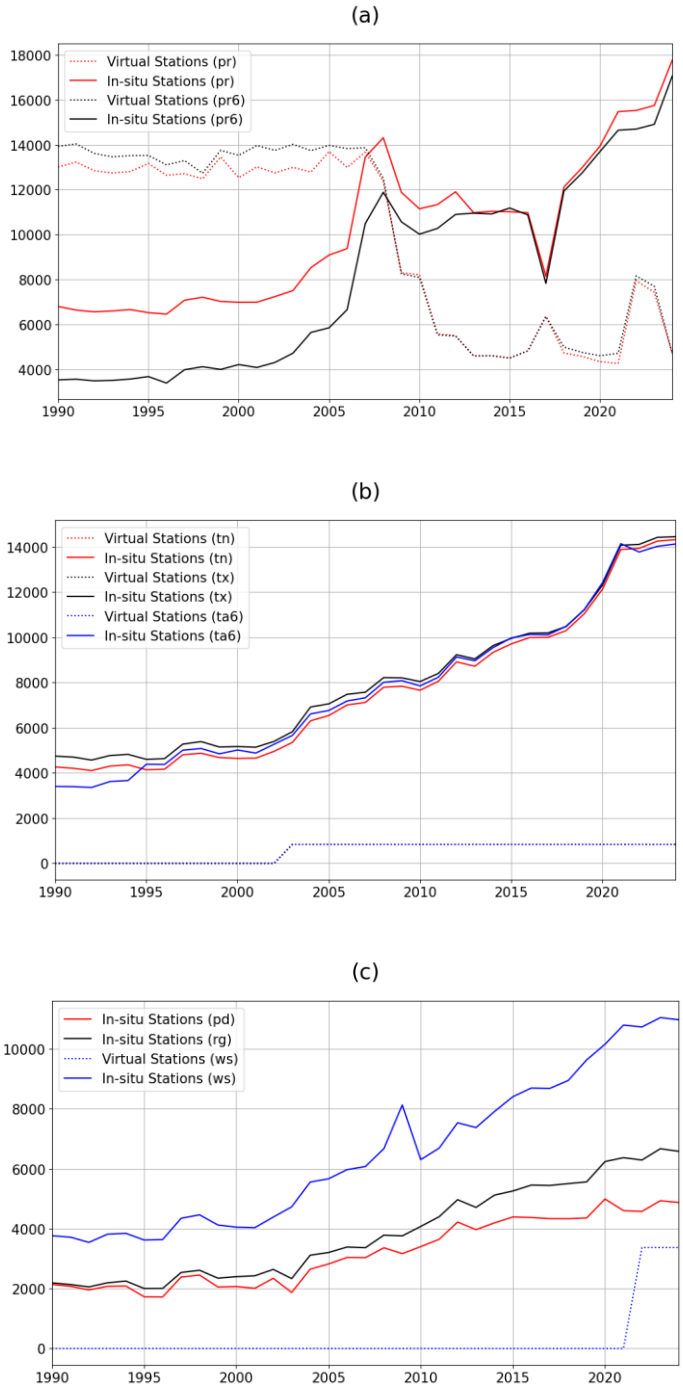

Figure 2 Number of stations over time used for interpolation in EMO-1 for the variables a) 6-hourly and daily total precip., b) minimum, maximum and 6-hourly average air temperature, and c) average wind speed, vapour pressure, and solar radiation. Solid lines denote the number of available in-situ stations over time. Dashed lines denote the number of virtual stations from the gridded datasets.

https://doi.org/10.5194/essd-2025-723
Preprint. Discussion started: 4 March 2026

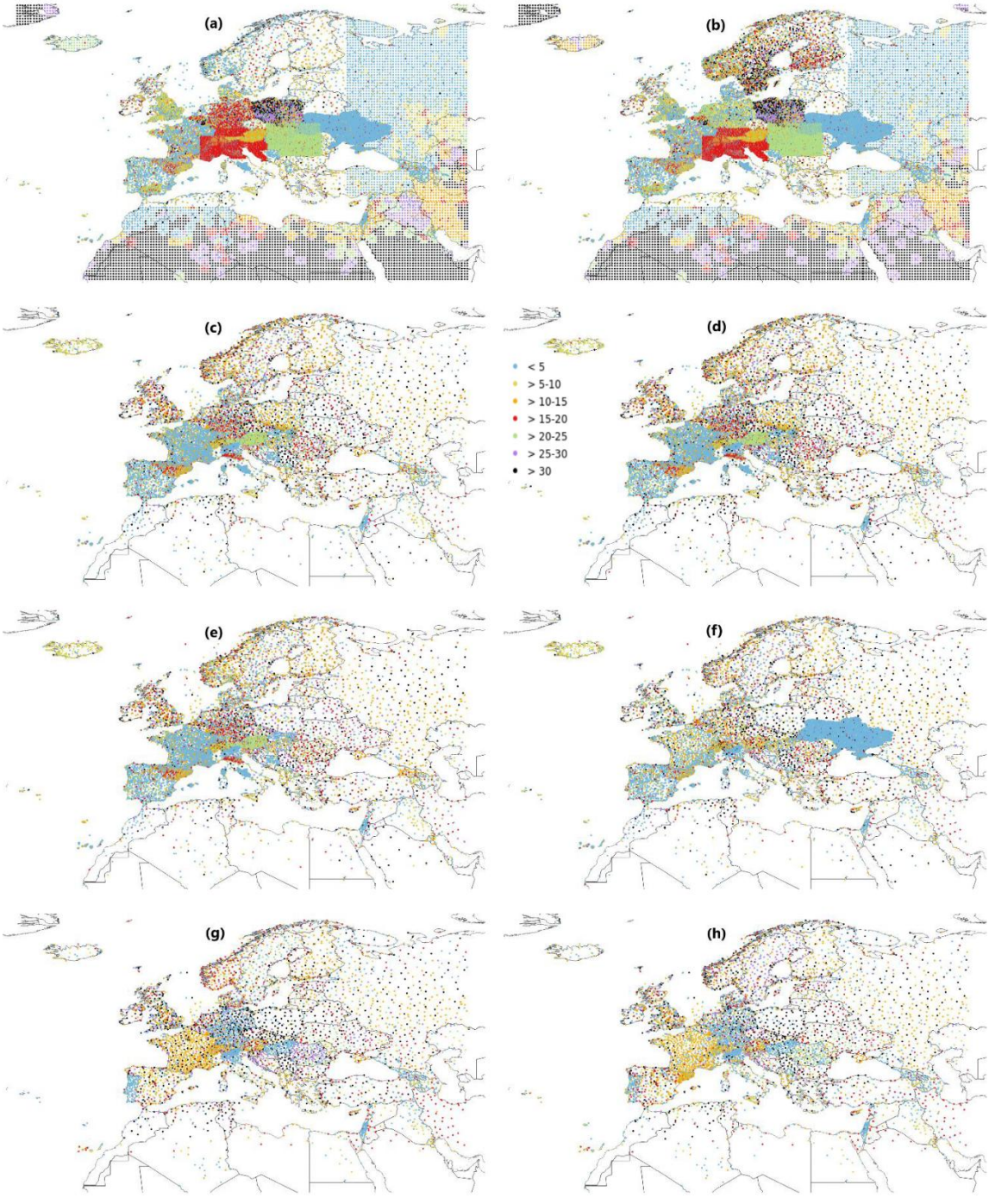

Figure 3 Spatial distribution of the number of stations used for interpolation in EMO-1 for the variables a) 6-hourly total precip., b) daily total precip., c) minimum temperature, d) maximum temperature, e) 6-hourly average air temperature, f) average wind speed, g) vapour pressure, and h) solar radiation. Colours indicate the record length.

https://doi.org/10.5194/essd-2025-723
Preprint. Discussion started: 4 March 2026

Figure 4 Availability of in-situ observations and gridded datasets for 6-hourly precipitation between 1990 – 2024 from data providers in EMO-1

https://doi.org/10.5194/essd-2025-723
Preprint. Discussion started: 4 March 2026

335

4 Data availability

The EMO-1 dataset is available in the JRC data catalogue: https://doi.org/10.2905/0BD84BE4-CEC8-4180-97A6-8B3ADAAC4D26 (Salamon et al., 2025).

The dataset is published under the Creative Commons Attribution 4.0 International (CC BY 4.0) licence.

340 Each of the 8 variables as indicated in Table 1 is stored in a separate folder. The 8 folders contain 34 files, each containing a full year of daily/6-hourly grids. Time stamps for the grids refer always to the end of the time interval. In addition, one folder containing the digital elevation model (DEM) used for height correction for the temperature interpolation and one folder with 8 sub-folders containing 34 files describing the station completeness are available. All the data share the same projection (WGS84) of grid and spatial resolution (1′). The files are stored in CF-1.6 compliant NetCDF format.

345 A README file provides further details related to the file structure, data description and general information. A CHANGELOG file provides a release history containing information about modification, bug-fixes, and updates performed for EMO-1. An annual update cycle of EMO-1 is foreseen to ensure that the dataset covers also more recent periods.

The open-source interpolation software (pyg2p) used for the interpolation of the meteorological observation is available at https://github.com/ec-jrc/pyg2p . Version 3.2.8 was used to generate EMO-1. Parsing of input files containing the observations

350 and producing the output in the required format a wrapper called *gridding* was used (https://github.com/ec-jrc/lisflood-utilities?tab=readme-ov-file#gridding).

5 Conclusions

We presented EMO-1, an operational, multi-variable gridded meteorological dataset for Europe that substantially advances EMO-5 in spatial detail, input data volume, method transparency and maintainability, while remaining tailored to the needs of

355 near-real-time hydrometeorological applications such as EFAS. EMO-1 increases the grid resolution from 5 km to 1-arc-minute (~1.5 km) on a WGS-84 latitude/longitude grid, extends the temporal coverage to 1990–2024 with annual updates, and ingests observations from 47 providers (41 station networks plus six gridded sources), representing a ~95 % increase over EMO-5. To mitigate data-sparse regions, selected high-resolution regional gridded products are incorporated as virtual stations.

360 The EMO-1 processing chain harmonizes heterogeneous reporting practices and temporal resolutions, aggregating to daily and 6-hourly targets following WMO conventions, with strict coverage requirements and a specific decumulation process of daily precipitation to 6-hourly totals to ensure the best possible representation of 6-hourly precipitation fields. A two-tier quality-control framework combines synchronous checks (season- and climate-zone-dependent thresholds, cross-variable

https://doi.org/10.5194/essd-2025-723
Preprint. Discussion started: 4 March 2026

consistency, and rate-of-change tests) with asynchronous diagnostics (flatliner detection, aggregation consistency, duplicate station resolution, and spatial/spatial-zero comparisons), thereby removing erroneous records before gridding.

EMO-1 replaces the proprietary SPHEREMAP scheme used in EMO-5 with an open-source implementation of Angular Distance Weighting (ADW), selected after cross-validated benchmarking against other deterministic interpolation methods. The methods displayed broadly similar skill; ADW provided slightly better performance for post-2010 6-hourly precipitation while remaining computationally efficient and robust for routine production.

The resulting dataset comprises eight variables (daily precipitation, 6-hourly precipitation, daily Tmin/Tmax, 6-hourly mean temperature, daily wind speed, solar radiation, and vapour pressure) over an extended pan-European domain. EMO-1 emphasizes information density and timeliness over long-term homogeneity in particular for precipitation and therefore making the dataset highly suitable for hydrological modelling, benchmarking, and continental-scale environmental services that require consistent, frequently updated forcings. However, the evolving station network yields spatial–temporal inhomogeneities that make the dataset less suitable for trend detection. In a future study we aim to provide a comparison of the new EMO-1 dataset with other gridded meteorological datasets such as the ENSEMBLES daily gridded observational dataset for Europe (E-OBS, Cornes et al., 2018), the reanalysis product ERA-5 (Hersbach et al, 2023) and the high-resolution pan-European hydrological reanalysis HERA (Tilloy et al., 2025).

The gridded meteorological data are openly available from the JRC Data Catalogue under CC BY 4.0, delivered as CF-1.6 NetCDF files (yearly stacks per variable) together with the DEM and station-completeness layers and are updated on an annual basis. The pyg2p interpolation codebase is publicly accessible to ensure reproducibility and future evolutions.

APPENDIX A

Table A1 List of in-situ data providers for EMO-1

Name	Parameter type				
	Precipitation	**Solar Radiation**	**Air temperature**	**Vapour pressure**	**Wind speed**
Agencia Estatal de Meteorología (Spain) [AEMET]	Dec 2019 - Dec 2024	Jan 2020 - Dec 2024	Dec 2019 - Dec 2024	-	Dec 2019 - Dec 2024
Deutscher Wetterdienst (Germany) [AMDASynop]	Sep 1995 - Jan 2008 Jan 2021 - Dec 2024	-	Jan 1990 - Dec 2024	-	Jan 1990 - Dec 2024

https://doi.org/10.5194/essd-2025-723
Preprint. Discussion started: 4 March 2026

Agenzia Regionale per la Protezione dell'Ambiente del Friuli Venezia Giulia (Italy) [ARPA-FVG]	Sep 1990 - Dec 2012 Jan 2014 - Dec 2024	Oct 1993 - Dec 2012 Jan 2014 - Dec 2024	Oct 1993 - Dec 2012 Jan 2014 - Dec 2024	-	Oct 1993 - Dec 2012 Jan 2014 - Dec 2024
Agenzia Regionale per la Prevenzione e l'Ambiente dell'Emilia-Romagna (Italy) [ARPASIM]	Jan 1990 - Dec 2024	Dec 2005 - Dec 2024	Jan 1990 - Dec 2024	-	Dec 2005 - Dec 2024
Slovenian Environment Agency [ARSO]	Dec 2003 - Apr 2004 Dec 2004 - Dec 2024	Jun 1993 - Dec 2024	Jun 1993 - Dec 2024	-	Jun 1993 - Dec 2024
Czech Hydro-Meteorological Institute [CHMI]	Jan 1998 - Dec 2024	-	Jan 1990 - Apr 1993 Jan 1996 - Dec 2024	-	-
Danish Meteorological Institute (Denmark & Greenland) [DMI]	Dec 2022 - Dec 2024	Dec 2022 - Dec 2024	Jan 2011 - Ago 2015 Nov 2015 - Dec 2024		Dec 2022 - Dec 2024
Deutscher Wetterdienst (global) [DWDSynop]	Jan 2018 - Dec 2024	Oct 1991 - Dec 2024	Jan 1990 - Dec 2024	-	Jan 1990 - Dec 2024
Environment Agency (England) [EA]	Sep 2018 - Dec 2024	-	-	-	-
Federal Hydrometeorological Institute (Bosnia-Herzegovina) [FHMZ]	Ago 2020 - Dec 2024	-	May 2020 - Dec 2024	-	Nov 2020 - Dec 2024
Finnish Meteorological Institute [FMI]	Jan 1990 - Dec 2024	-	Jan 2010 - Dec 2024	-	Jan 2010 - Dec 2024

https://doi.org/10.5194/essd-2025-723
Preprint. Discussion started: 4 March 2026

Hydrological Information Centre (HIC) - Flanders Hydraulics Research (Belgium) [HIC]	May 2008 - Dec 2024	-	-	-	-
Hungarian Meteorological Service [HMS]	Jan 1997 - Dec 2008 Jan 2021 - Dec 2024	Jan 2021 - Dec 2024	Jan 1997 - Dec 2008 Jan 2021 - Dec 2024	-	Jan 1997 - Dec 2008 Jan 2021 - Dec 2024
Institute of Meteorology and Water Management (Poland)* [IMGW]	Jan 1990 - Dec 2024	-	Jan 1990 - Dec 2024	Jan 1990 - Mar 2020	Jan 1990 - Dec 2024
Israel Meteorological Service [IMS]	Oct 2020 - Dec 2024	Oct 2020 - Dec 2024	Oct 2020 - Dec 2024	-	Oct 2020 - Dec 2024
Institute for Ocean and Atmosphere (Portugal) [IPMA]	Jan 2000 - Mar 2024 Jul 2024 - Dec 2024	Jan 2000 - Mar 2024 Jul 2024 - Dec 2024	Jan 2000 - Mar 2024 Jul 2024 - Dec 2024	-	Jan 2001 - Mar 2024 Jul 2024 - Dec 2024
Kosovo Hydrometeorological Institute [KHMI]	Sep 2014 - Dec 2024	Jan 2019 - Dec 2024	Sep 2014 - Dec 2024	-	Jan 2018 - Dec 2024
Royal Netherlands Meteorological Institute [KNMI]	Apr 2020 - Dec 2024	Apr 2020 - Dec 2024	Apr 2020 - Dec 2024	-	Apr 2020 - Dec 2024
Agenzia Regionale Di Protezione Civile (Lazio, Italy) [Lazio]	Nov 2020 - Dec 2024	Nov 2020 - Dec 2024	Nov 2020 - Dec 2024	-	Nov 2020 - Dec 2024
National Environmental Agency (Georgia) [LEPL]	Jan 1993 - Dec 2019 Mar 2020 - Dec 2024	-	Jan 1993 - Dec 2024	-	Mar 2020 - Dec 2024
Agenzia Regionale per la Protezione dell'Ambiente (Lombardia, Italy)	Mar 2024 - Dec 2024	-	-	-	-

https://doi.org/10.5194/essd-2025-723
Preprint. Discussion started: 4 March 2026

Wageningen Environmental Research (ALTERRA)* [MARS]	Jan 1990 - Dec 2024	Jan 1990 - Dec 2024	Jan 1990 - Dec 2024	Jan 1990 - Dec 2024	Jan 1990 - Dec 2024
MeteoFrance	Jan 1990 - Dec 2024	Dec 2021 - Dec 2024	Jan 1990 - Dec 2024	-	Jan 1990 - Dec 2024
MeteoLux (Luxemburg)	Jan 1996 - Nov 2000 Oct 2012 - Dec 2024	-	Jan 1996 - Dec 2024	-	Jan 1996 - Dec 2024
MeteoSchweiz (Switzerland) [MeteoSwiss]	Jan 1990 - Dec 2024	Jan 1990 - Dec 2024	Jan 1990 - Dec 2024	-	Jan 1990 - Dec 2024
Met Éireann (Ireland) [METIE]	Jan 1990 - Dec 2024	Jan 2022 - Dec 2024	Jan 1990 - Dec 2024	-	Jan 1990 - Dec 2024
Norwegian Meteorological Institute [NMI]	Jan 1990 - Dec 2024	-	Jan 1990 - Dec 2024	-	Jan 1990 - Dec 2024
Agenzia Regionale per la Protezione Ambientale del Piemonte (Italy)	Nov 2024 - Dec 2024	-	-	-	-
Republic Hydrometeorological Service of the Republic of Srpska (Bosnia and Herzegovina) [RHMZRS]	Jan 2021 - Dec 2024	-	Jan 2021 - Dec 2024	-	-
Automatic System of Hydrological Information (SAIH) for the Ebro river basin (Spain) [SAIH]	Jan 1997 - Dec 2024	Apr 2008 - Dec 2024	Jul 2001 - Dec 2024	-	Apr 2008 - Dec 2024
Automatic System of Hydrological Information (SAIH) for the Guadalquivir river basin (Spain)	Oct 1999 - Dec 2024	-	-	-	-

https://doi.org/10.5194/essd-2025-723
Preprint. Discussion started: 4 March 2026

Slovak Hydro-Meteorological Institute [SHMU]	Jan 2004 - Feb 2008 Jul 2008 - Dec 2024	-	May 2021 - Dec 2024	-	-
Servei Meteorològic de Catalunya (Spain) [SMC]	Jan 2009 - Dec 2024	Jan 2009 - Dec 2024	Jan 2009 - Dec 2024	-	May 2009 - Dec 2024
Swedish Meteorological and Hydrological Institute [SMHI]	Jan 1990 - Dec 2024	Jan 2008 - Dec 2024	Jan 1990 - Dec 2024	-	Jan 1990 - Dec 2024
Service public de Wallonie (Belgium) [SPW]	Jan 1990 - Dec 2021 Oct 2022 - Dec 2024	-	-	-	-
Flanders Environment Agency (Belgium) [VMM]	May 2004 - Dec 2024	-	May 2004 - Dec 2024	-	Oct 2001 - Dec 2024
Hellenic National Meteorological Service* [HNMS]	Jan 1990 - Dec 2000	-	Jan 1990 - Dec 2000	Jan 1990 - Dec 2000	Jan 1990 - Dec 2000
ECA	Jan 1990 - Feb 2012	-	-	-	-
Meteo Consult	Dec 2007 - Sep 2016	-	-	-	-
Euro Synop	Feb 2003 - May 2009	-	Feb 2003 - May 2009	-	Feb 2003 - May 2009
Danube	-	-	Jan 1991 - Dec 2003	-	-

* Denotes data providers where daily precipitation values have been decumulated to obtain 6-hourly precipitation values

Table A2 List of gridded datasets used in EMO-1

Name	Parameter type	Time period

https://doi.org/10.5194/essd-2025-723
Preprint. Discussion started: 4 March 2026

	Precipitation	**Air temperature**	**Wind speed**	
GeoSphere Austria INCA (Haiden et al., 2011) [ZAMG]	Jan 2003 - Dec 2024	Jan 2003 - Dec 2024	-	January 2003 – December 2023
EURO4M-APGD* (Isotta et al., 2014)	Jan 1990 - Dec 2008	-	-	January 1990 – December 2008
CarpatClim* (Spinoni et al., 2015)	Jan 1990 - Dec 2010	-	-	January 1990 – December 2010
CombiPrecip (Federal Office of Meteorology and Climatology MeteoSuisse)	Jun 2017 - Dec 2024	-	-	June 2017 – December 2023
ERA-5 Land (C3S, 2019)	Jan 1990 - Sep 2023	-	-	January 1990 – September 2023
ICON Numerical Weather Predictions (German Weather Service)	March 2022 - Dec 2024	-	March 2022 – December 2023	March 2022 – December 2023

390

* Denotes data providers where daily precipitation values have been decumulated to obtain 6-hourly precipitation values

https://doi.org/10.5194/essd-2025-723
Preprint. Discussion started: 4 March 2026

Open Access Earth System Science Data Discussions

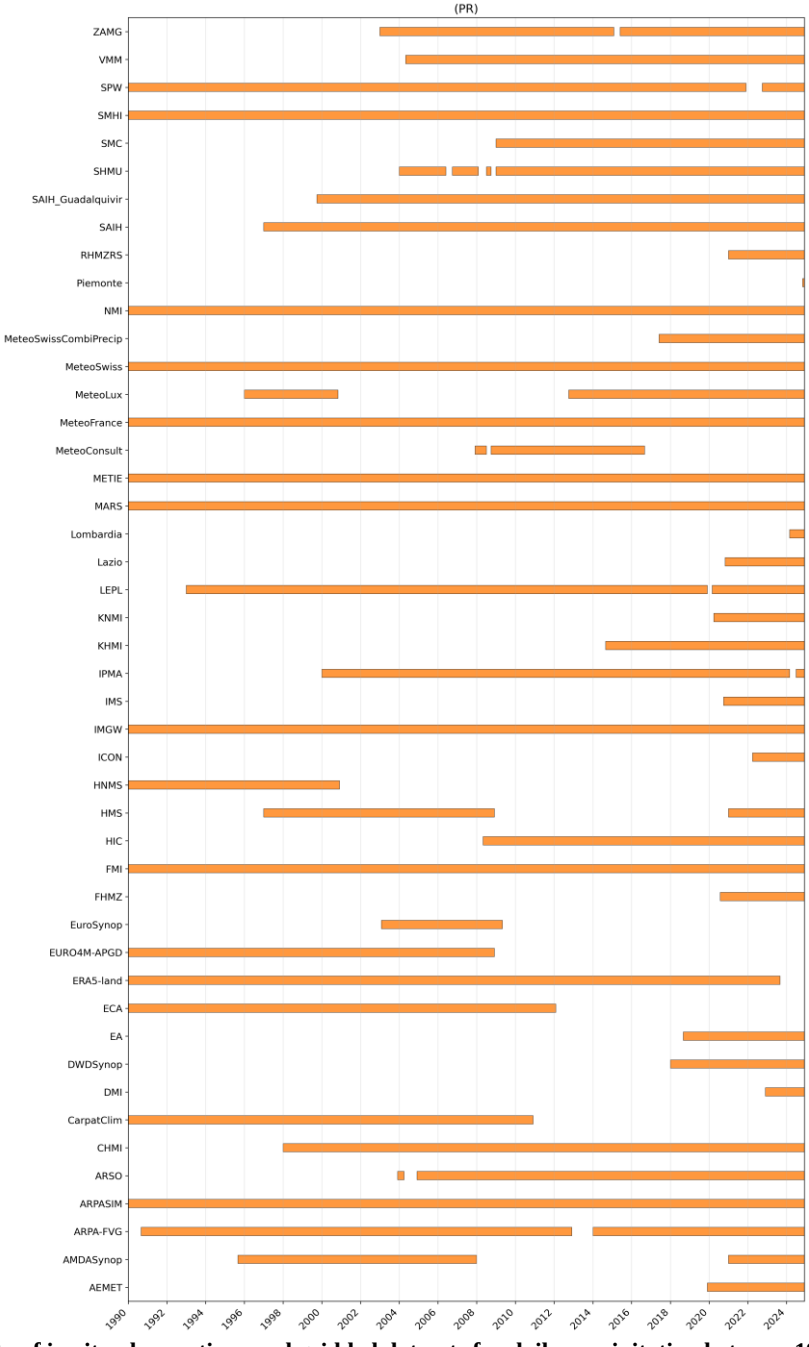

Figure A1 Availability of in-situ observations and gridded datasets for daily precipitation between 1990 – 2024 from data providers in EMO-1

395

https://doi.org/10.5194/essd-2025-723
Preprint. Discussion started: 4 March 2026

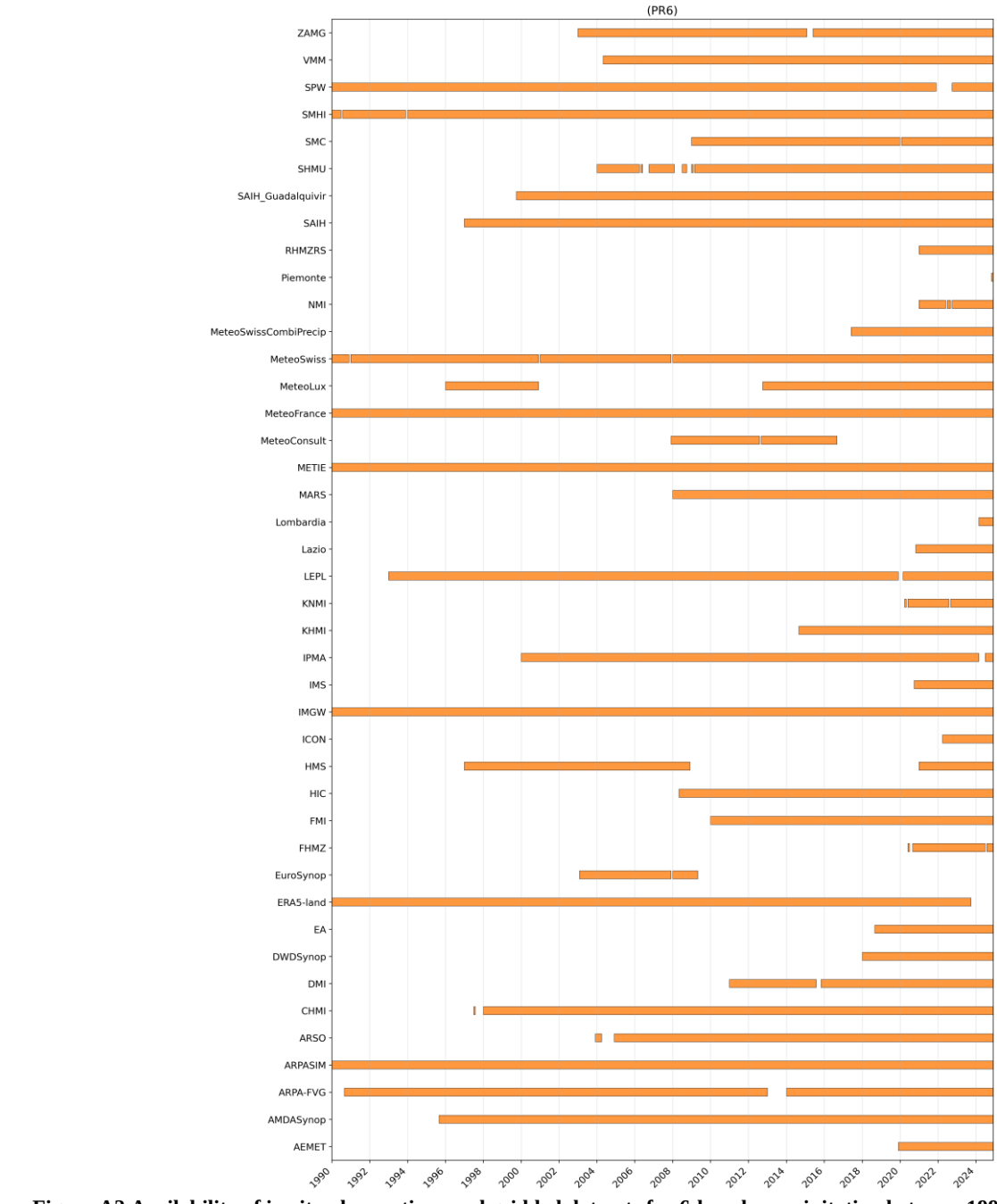

Figure A2 Availability of in-situ observations and gridded datasets for 6-hourly precipitation between 1990 – 2024 from data providers in EMO-1

https://doi.org/10.5194/essd-2025-723
Preprint. Discussion started: 4 March 2026

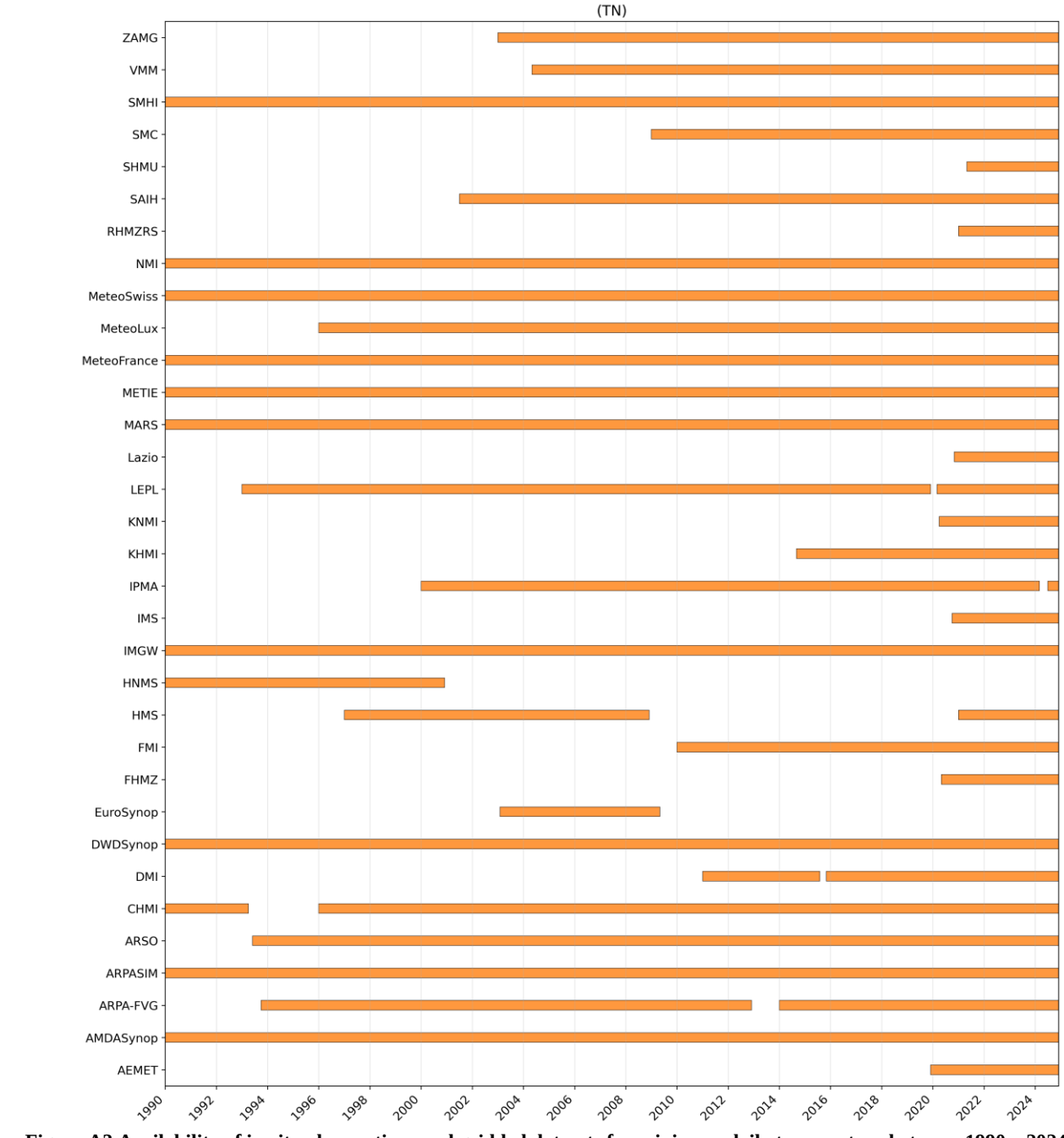

Figure A3 Availability of in-situ observations and gridded datasets for minimum daily temperature between 1990 – 2024 from data providers in EMO-1

https://doi.org/10.5194/essd-2025-723
Preprint. Discussion started: 4 March 2026

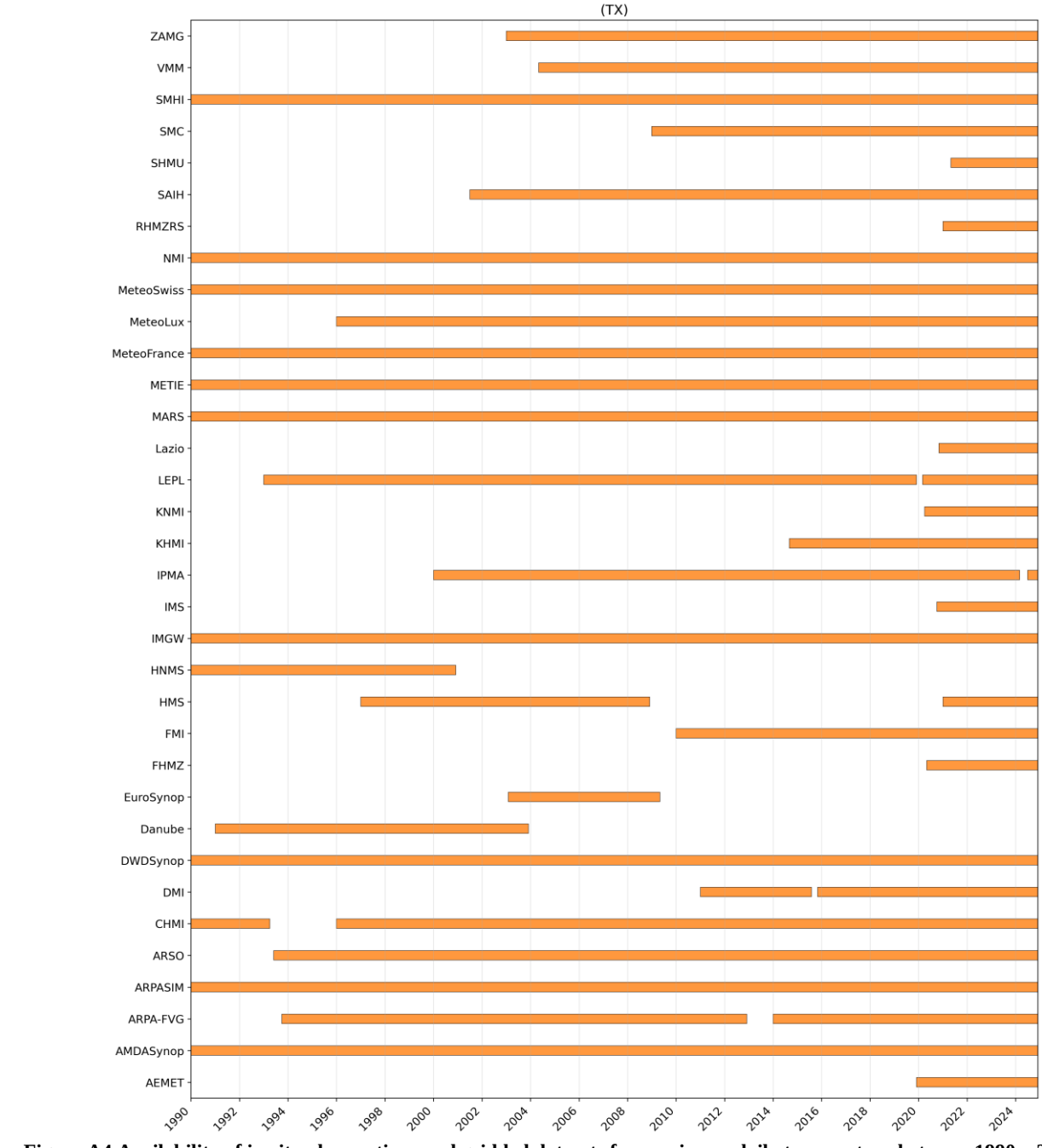

Figure A4 Availability of in-situ observations and gridded datasets for maximum daily temperature between 1990 – 2024 from data providers in EMO-1

https://doi.org/10.5194/essd-2025-723
Preprint. Discussion started: 4 March 2026

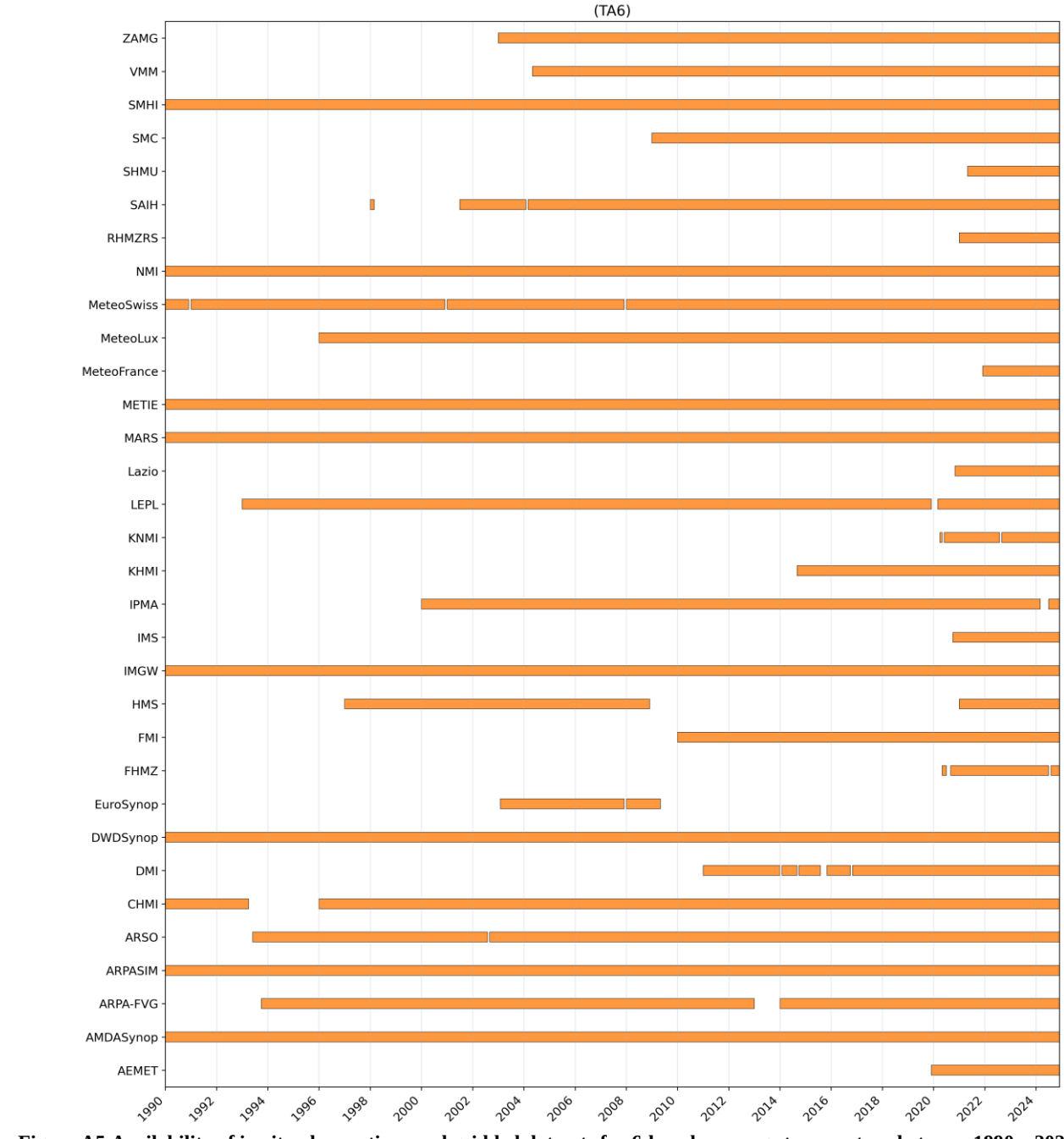

Figure A5 Availability of in-situ observations and gridded datasets for 6-hourly average temperature between 1990 – 2024 from data providers in EMO-1

https://doi.org/10.5194/essd-2025-723
Preprint. Discussion started: 4 March 2026

Figure A6 Availability of in-situ observations and gridded datasets for daily average windspeed between 1990 – 2024 from data providers in EMO-1

415

https://doi.org/10.5194/essd-2025-723
Preprint. Discussion started: 4 March 2026

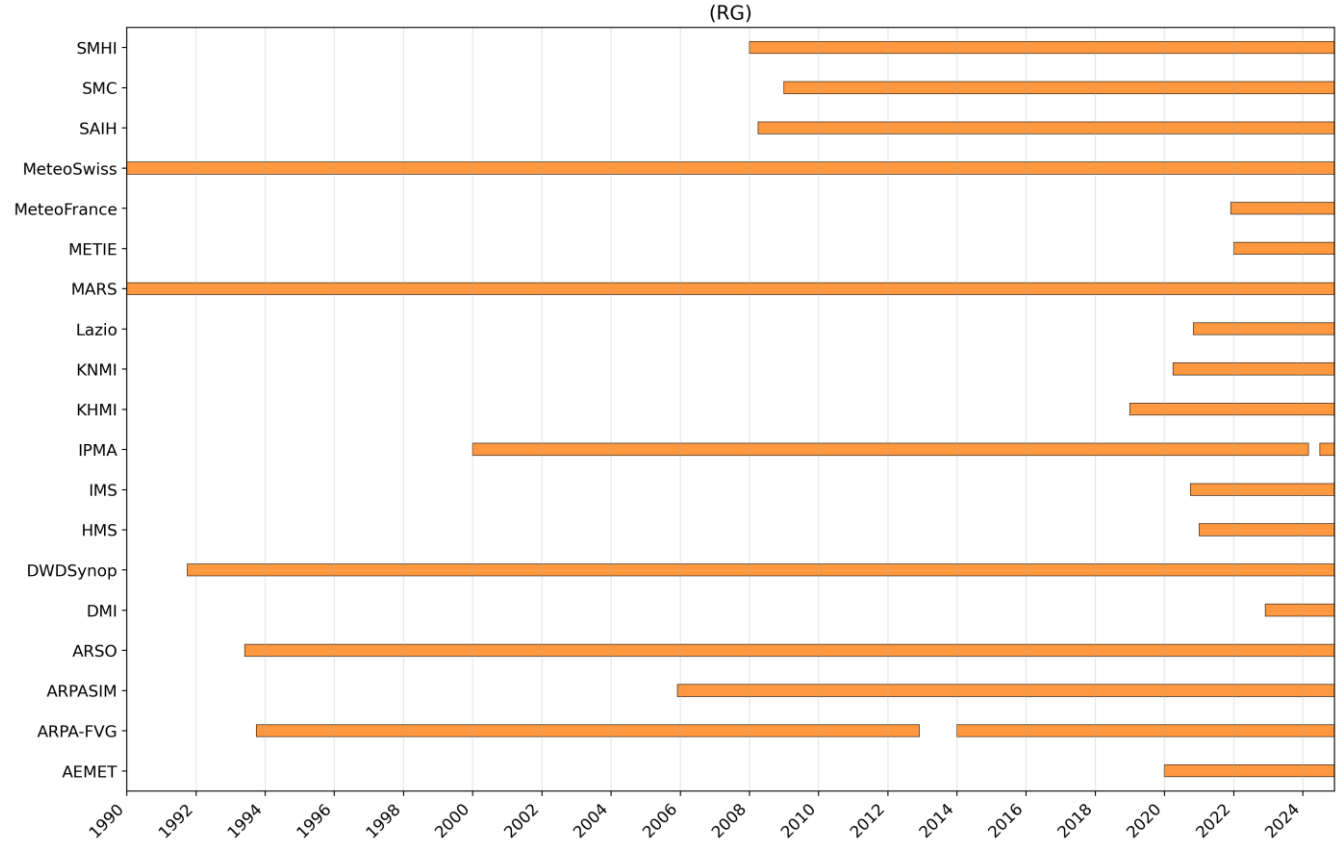

Figure A7 Availability of in-situ observations for daily solar radiation between 1990 – 2024 from data providers in EMO-1

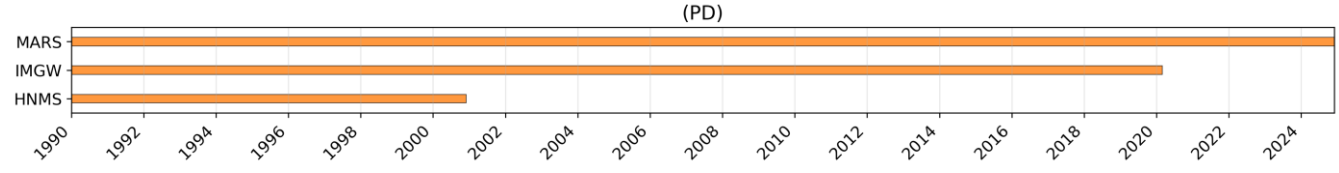

Figure A8 Availability of in-situ observations for daily vapour pressure between 1990 – 2024 from data providers in EMO-1

https://doi.org/10.5194/essd-2025-723
Preprint. Discussion started: 4 March 2026

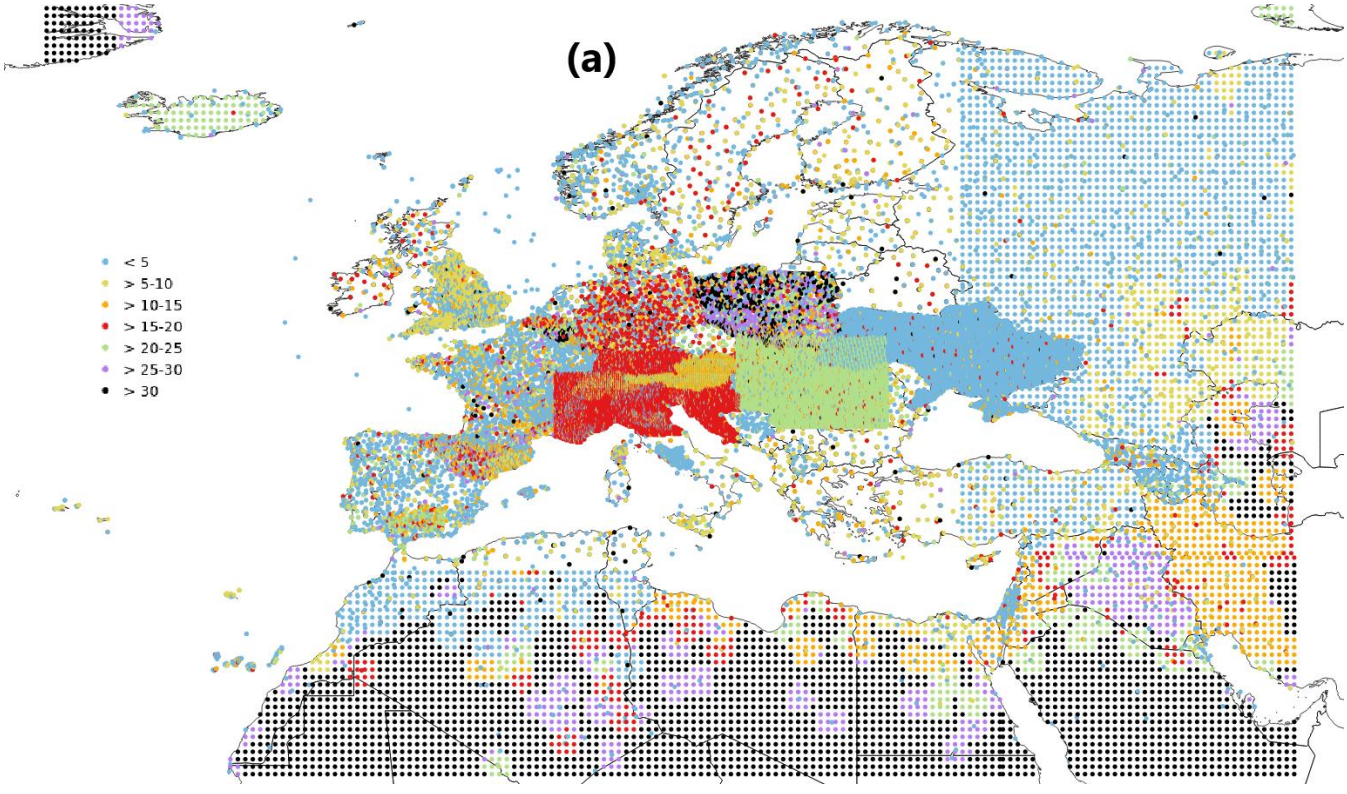

Figure A9 Spatial distribution of the number of stations used for interpolation in EMO-1 for the variable a) 6-hourly precipitation. Colours indicate the record length.

https://doi.org/10.5194/essd-2025-723
Preprint. Discussion started: 4 March 2026

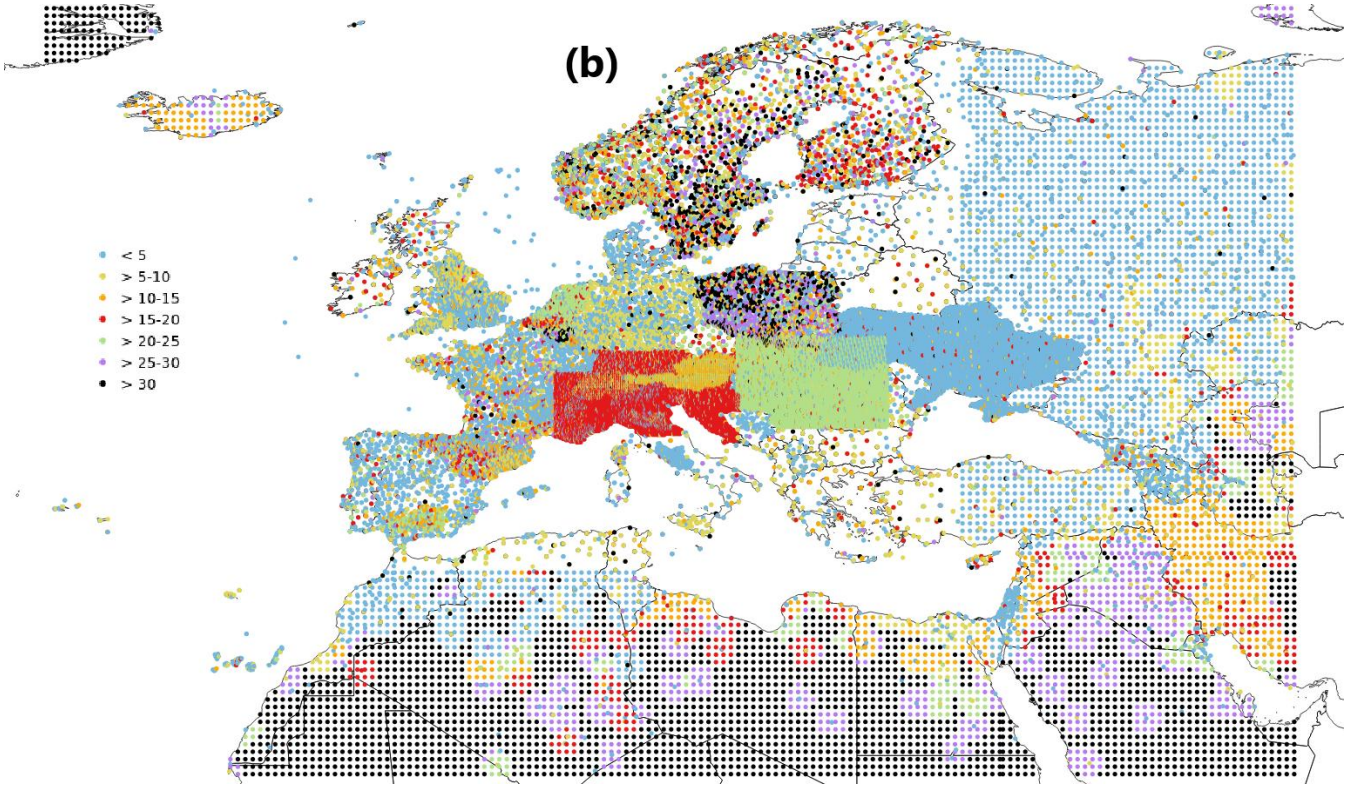

Figure A10 Spatial distribution of the number of stations used for interpolation in EMO-1 for the variable b) daily precipitation. Colours indicate the record length.

https://doi.org/10.5194/essd-2025-723
Preprint. Discussion started: 4 March 2026

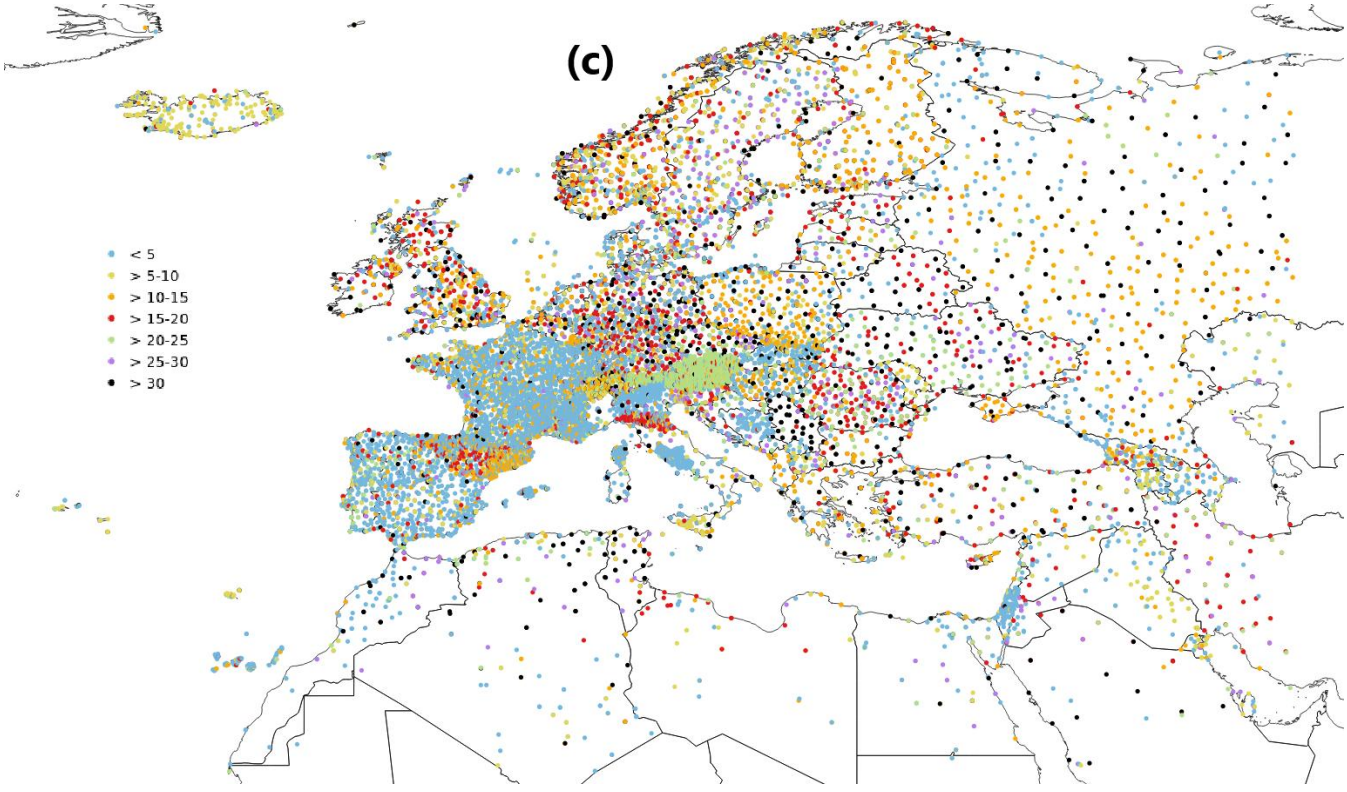

Figure A11 Spatial distribution of the number of stations used for interpolation in EMO-1 for the variable c) daily minimum temperature. Colours indicate the record length.

https://doi.org/10.5194/essd-2025-723
Preprint. Discussion started: 4 March 2026

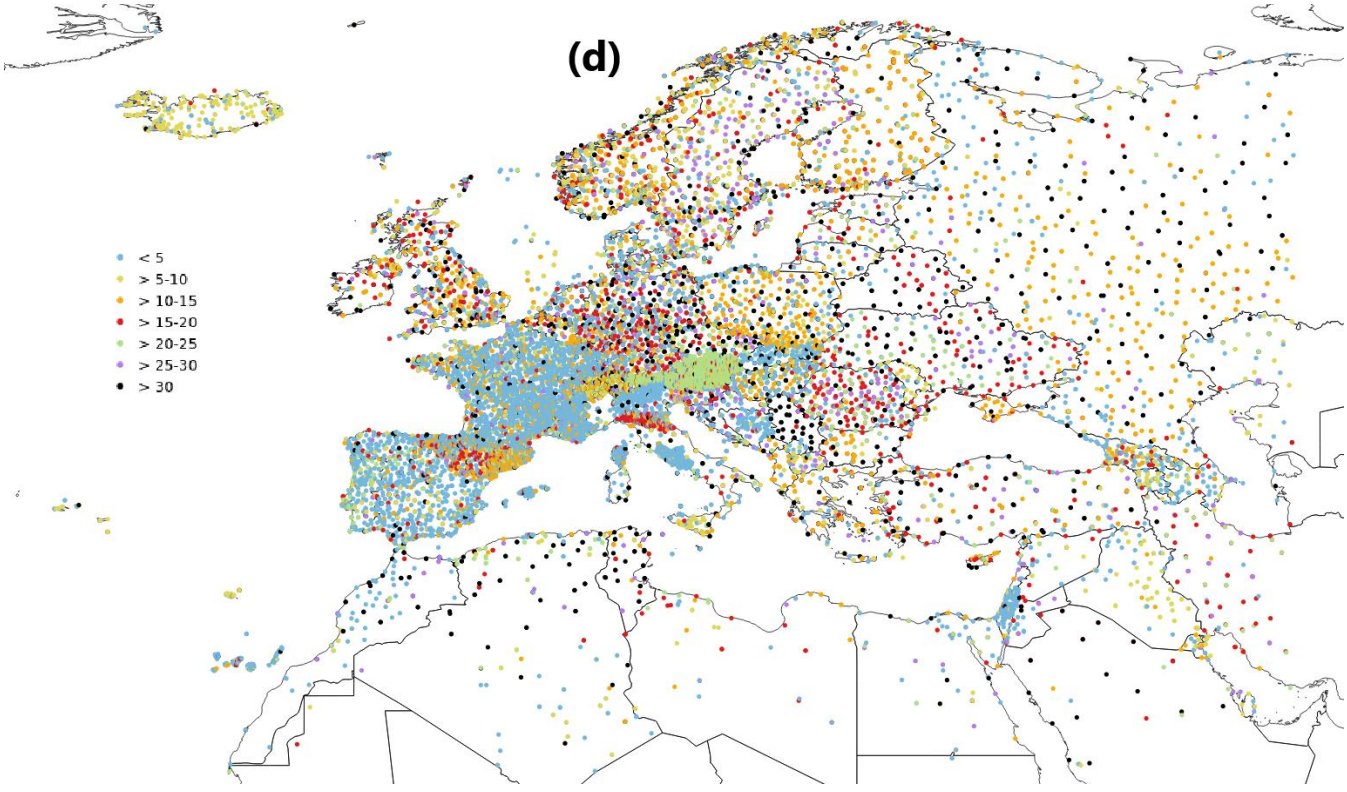

Figure A12 Spatial distribution of the number of stations used for interpolation in EMO-1 for the variable d) daily maximum temperature. Colours indicate the record length.

https://doi.org/10.5194/essd-2025-723
Preprint. Discussion started: 4 March 2026

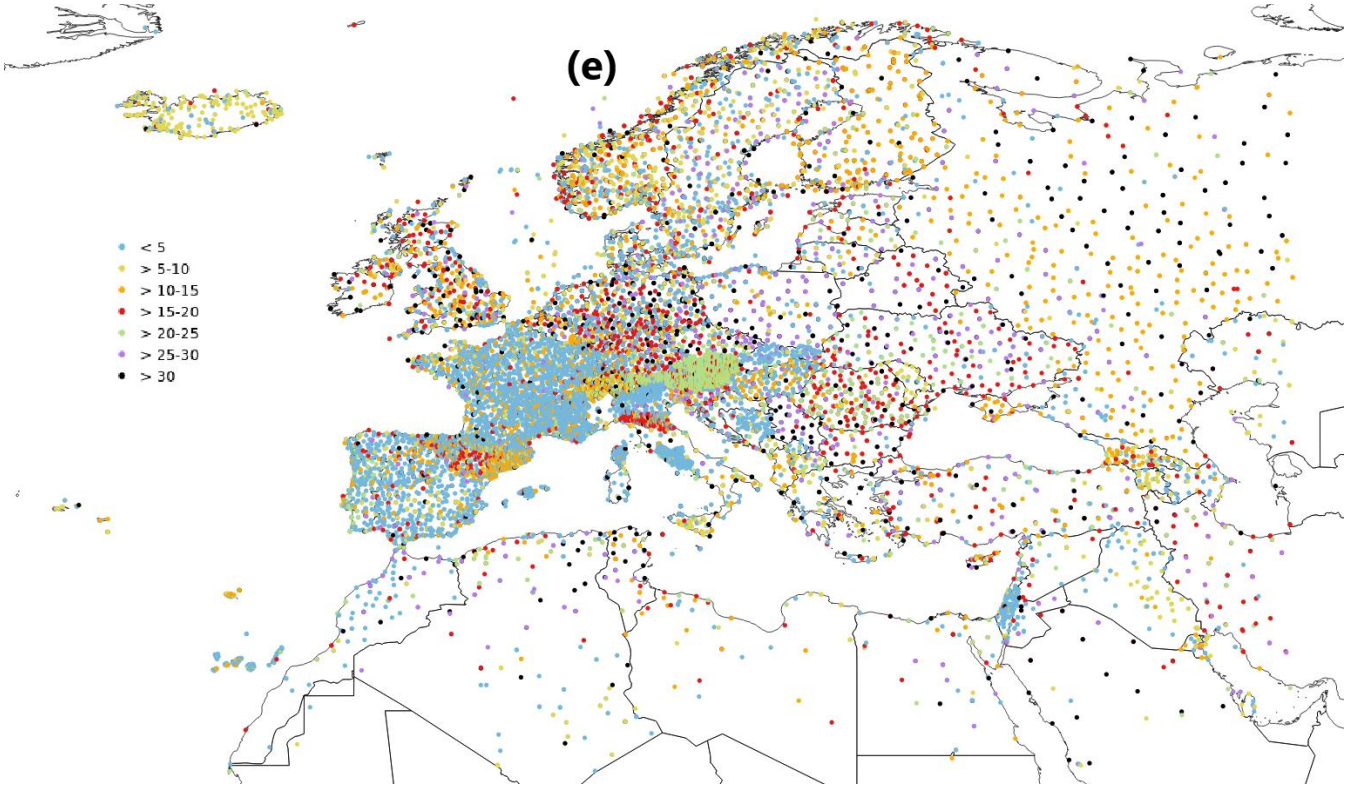

Figure A13 Spatial distribution of the number of stations used for interpolation in EMO-1 for the variable e) 6-hourly average temperature. Colours indicate the record length.

https://doi.org/10.5194/essd-2025-723
Preprint. Discussion started: 4 March 2026

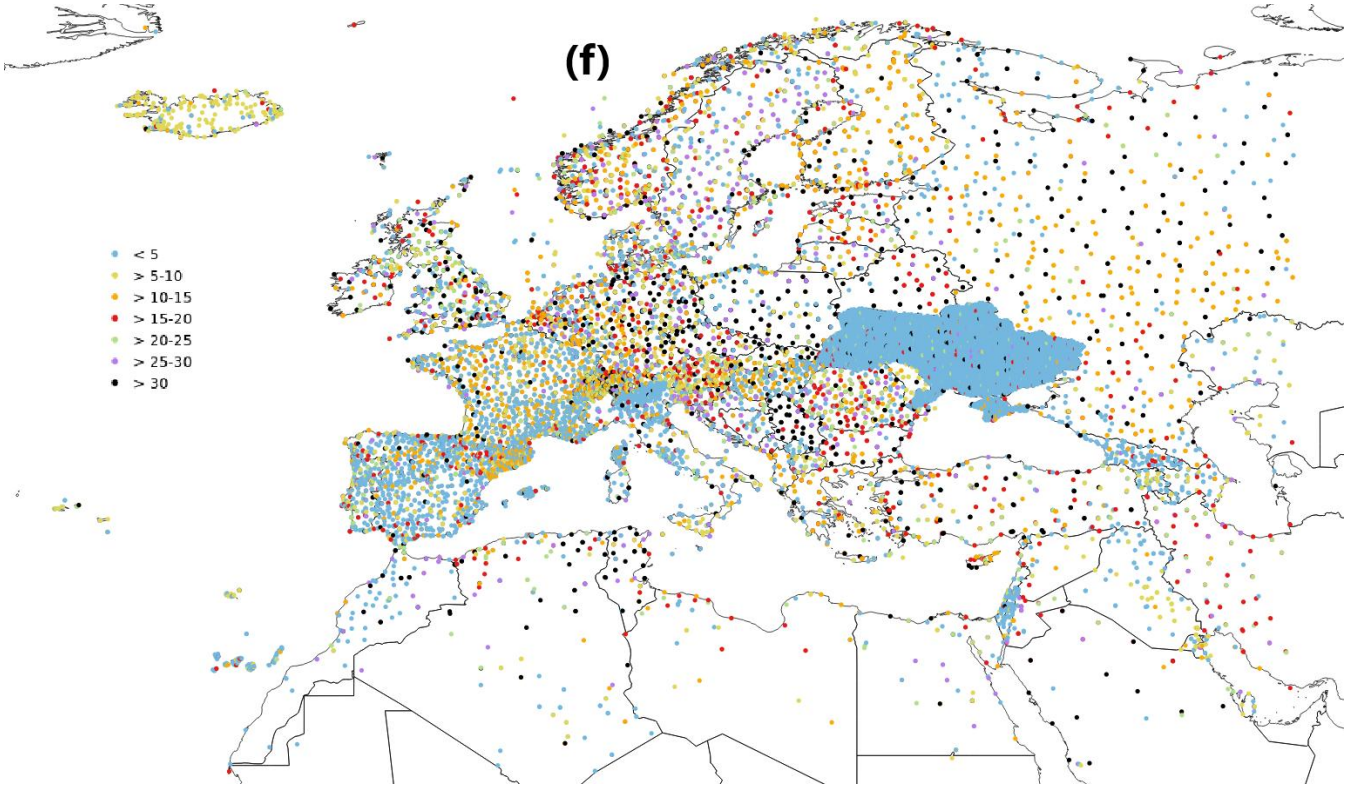

Figure A14 Spatial distribution of the number of stations used for interpolation in EMO-1 for the variable f) average windspeed. Colours indicate the record length.

https://doi.org/10.5194/essd-2025-723
Preprint. Discussion started: 4 March 2026

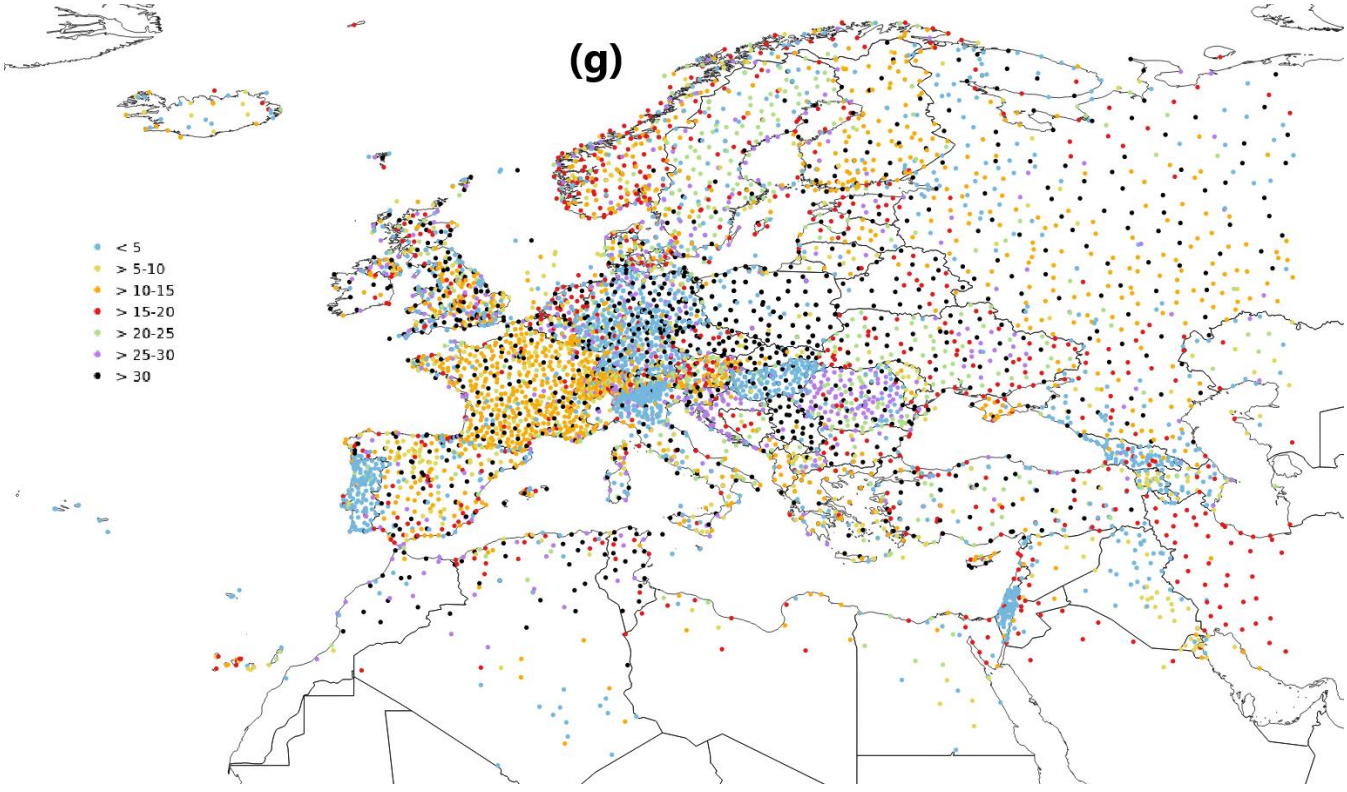

Figure A15 Spatial distribution of the number of stations used for interpolation in EMO-1 for the variable g) vapour pressure. Colours indicate the record length.

https://doi.org/10.5194/essd-2025-723
Preprint. Discussion started: 4 March 2026

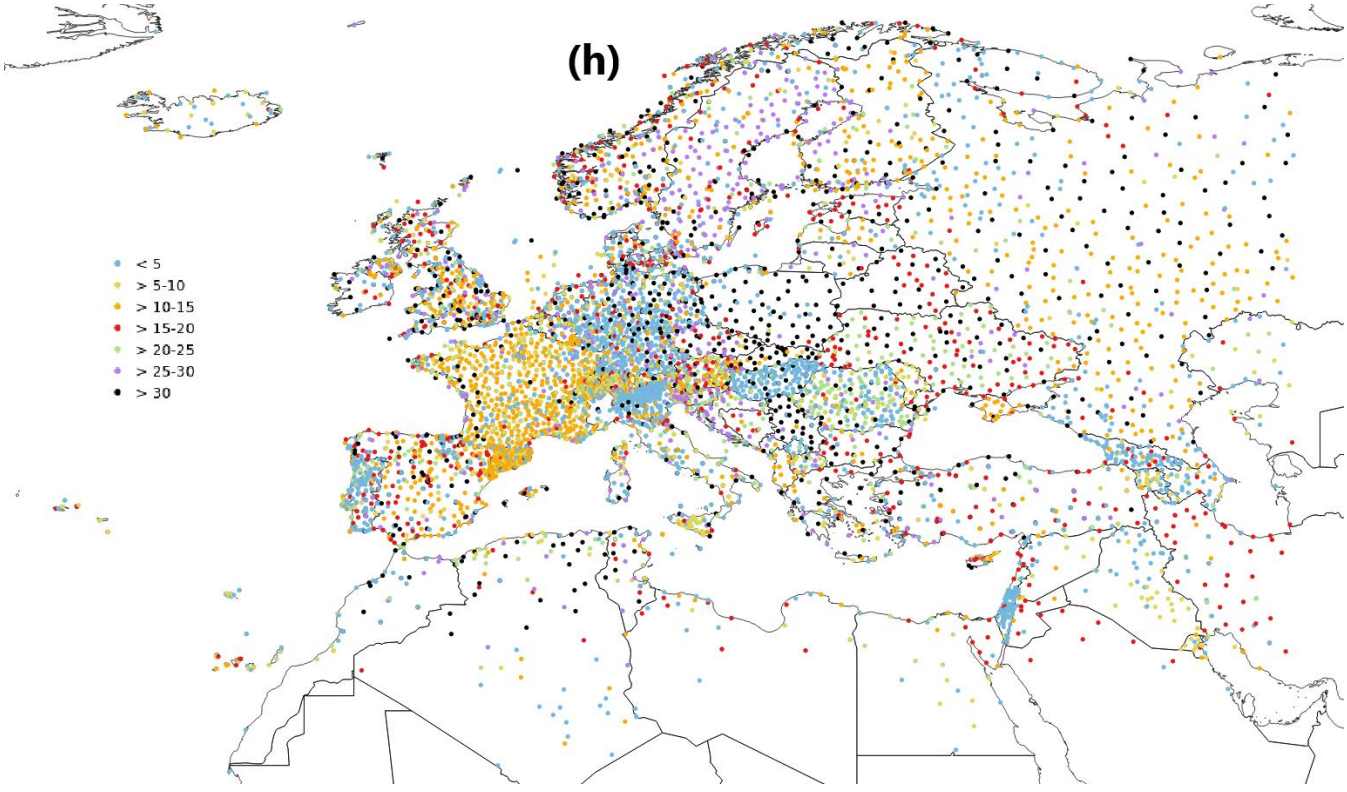

Figure A16 Spatial distribution of the number of stations used for interpolation in EMO-1 for the variable h) solar radiation. Colours indicate the record length.

445

https://doi.org/10.5194/essd-2025-723
Preprint. Discussion started: 4 March 2026

Open Access Earth System Science Data Discussions

APPENDIX B

Table B1 6-hourly total precipitation: MAE for dates before 2008, for increasing threshold values of observed precipitation. Best values are highlighted in bold

Minimum value of observed precipitation	ADW	CDD
1mm	0.943	**0.909**
10 mm	4.517	**4.440**
25 mm	**15.270**	15.849
50 mm	**45.539**	46.379
75 mm	**82.449**	85.545

Table B2 6-hourly mean temperature: summary of error measures for the selected interpolation schemes. Best values are highlighted in bold.

	Spheremap	ADW
MAE (K)	0.959	**0.953**
MSE (K^2)	**2.421**	2.442
MBE (or ME) (K)	**-0.016**	0.028
R (-)	0.959	0.959

Table B3 Daily minimum temperature: summary of error measures for the selected interpolation schemes. Best values are highlighted in bold.

	Spheremap	ADW
MAE (K)	0.855	**0.845**
MSE (K^2)	2.009	**1.200**
MBE (or ME) (K)	**-0.016**	0.020
R (-)	0.952	0.952

Table B4 Daily maximum temperature: summary of error measures for the selected interpolation schemes. Best values are highlighted in bold.

	Spheremap	ADW
MAE (K)	0.903	**0.901**
MSE (K^2)	**2.134**	2.147
MBE (or ME) (K)	**-0.019**	0.023
R (-)	0.976	0.976

https://doi.org/10.5194/essd-2025-723
Preprint. Discussion started: 4 March 2026

Table B5 Daily mean wind speed: summary of error measures for the selected interpolation schemes. Best values are highlighted in bold

	Spheremap	ADW
MAE (m/s)	0.725	**0.702**
MSE (m^2/s^2)	1.989	**1.961**
MBE (or ME) (m/s)	0.046	**0.037**
R (-)	0.805	**0.811**

Table B6 Daily mean vapour pressure: summary of error measures for the selected interpolation schemes. Best values are highlighted in bold.

	Spheremap	ADW
MAE (hPa)	**0.970**	0.973
MSE (hPa^2)	**2.652**	2.687
MBE (ME) (hPa)	0.010	**0.009**
R (-)	**0.894**	0.893

Acknowledgements

We gratefully acknowledge the financial support provided by the Copernicus programme and in particular by the Copernicus Emergency Management Service. Furthermore, we would like to thank all the data providers for their cooperation and for providing the in-situ observations.

AI tools have been used only to support the drafting of the abstract of the manuscript.

References

Adler, R.F., Sapiano, M.R.P., Huffman, G.J., Wang, J.-J., Gu, G., Bolvin, D., Chiu, L., Schneider, U., Becker, A., Nelkin, E.: The Global Precipitation Climatology Project (GPCP) Monthly Analysis (New Version 2.3) and a Review of 2017 Global Precipitation, Atmosphere, *9*, 138, https://doi.org/10.3390/atmos9040138, 2018.

Becker, A., Finger, P., Meyer-Christoffer, A., Rudolf, B., Schamm, K., Schneider, U., and Ziese, M.: A description of the global land-surface precipitation data products of the Global Precipitation Climatology Centre with sample applications

including centennial (trend) analysis from 1901–present, Earth Syst. Sci. Data, 5, 71–99, https://doi.org/10.5194/essd-5-71-2013, 2013.

Camera, C., Bruggeman, A., Hadjinicolaou, P., Pashiardis, S., & Lange, M. A.: Evaluation of interpolation techniques for the creation of gridded daily precipitation (1 × 1 km2), Cyprus, 1980–2010. Journal of Geophysical Research, 119(2), 693–712. https://doi.org/10.1002/2013JD020611, 2014.

Choulga, M., Moschini, F., Mazzetti, C., Grimaldi, S., Disperati, J., Beck, H., Salamon, P., and Prudhomme, C.: Technical note: Surface fields for global environmental modelling, Hydrol. Earth Syst. Sci., 28, 2991–3036, https://doi.org/10.5194/hess-28-2991-2024, 2024.

Contractor, S., Donat, M. G., Alexander, L. V., Ziese, M., Meyer-Christoffer, A., Schneider, U., Rustemeier, E., Becker, A., Durre, I., and Vose, R. S.: Rainfall Estimates on a Gridded Network (REGEN) – a global land-based gridded dataset of daily precipitation from 1950 to 2016, Hydrol. Earth Syst. Sci., 24, 919–943, https://doi.org/10.5194/hess-24-919-2020 , 2020.

Cornes, R. C., van der Schrier, G., van den Besselaar, E. J. M., & Jones, P. D.: An ensemble version of the E-OBS temperature and precipitation data sets, Journal of Geophysical Research: Atmospheres, 123, 9391–9409. https://doi.org/10.1029/2017JD028200, 2018.

Copernicus Climate Change Service (C3S): ERA5-Land hourly data from 1950 to present, Copernicus Climate Change Service Climate Data Store (CDS). DOI: 10.24381/cds.e2161bac, 2019.

Copernicus Climate Change Service (C3S) and World Meteorological Organization (WMO): European State of the Climate 2024, climate.copernicus.eu/ESOTC/2024, doi.org/10.24381/14j9-s541, 2025.

Doblas-Reyes, F.J., A.A. Sörensson, M. Almazroui, A. Dosio, W.J. Gutowski, R. Haarsma, R. Hamdi, B. Hewitson, W.-T. Kwon, B.L. Lamptey, D. Maraun, T.S. Stephenson, I. Takayabu, L. Terray, A. Turner, and Z. Zuo: Linking Global to Regional Climate Change. In Climate Change 2021: The Physical Science Basis. Contribution of Working Group I to the Sixth Assessment Report of the Intergovernmental Panel on Climate Change [Masson-Delmotte, V., P. Zhai, A. Pirani, S.L. Connors, C. Péan, S. Berger, N. Caud, Y. Chen, L. Goldfarb, M.I. Gomis, M. Huang, K. Leitzell, E. Lonnoy, J.B.R. Matthews, T.K. Maycock, T. Waterfield, O. Yelekçi, R. Yu, and B. Zhou (eds.)]. Cambridge University Press, Cambridge, United Kingdom and New York, NY, USA, pp. 1363–1512, doi:10.1017/9781009157896.012, 2021.

https://doi.org/10.5194/essd-2025-723
Preprint. Discussion started: 4 March 2026

Dosio, A.: Projections of climate change indices of temperature and precipitation from an ensemble of bias-adjusted high-resolution EURO-CORDEX regional climate models, J. Geophys. Res. Atmos., 121, 5488–5511, doi:10.1002/2015JD024411, 2016.

Dosio, A., Pinto, I., Lennard, C., Sylla, M. B., Jack, C., Nikulin, G.: What can we know about recent past precipitation over Africa? daily characteristics of African precipitation from a large ensemble of observational products for model evaluation, Earth and Space Science, 8, e2020EA001466. https://doi.org/10.1029/2020EA001466, 2021.

Haiden, T., Kann, A., Wittmann, C., Pistotnik, G., Bica, B., Gruber, C.: The integrated nowcasting through comprehensive analysis (INCA) system and its validation over the Eastern Alpine region, Weather and Forecasting, 26, 2, 166-183, https://doi.org/10.1175/2010WAF2222451.1, 2011.

Hersbach, H., Bell, B., Berrisford, P., Biavati, G., Horányi, A., Muñoz Sabater, J., Nicolas, J., Peubey, C., Radu, R., Rozum, I., Schepers, D., Simmons, A., Soci, C., Dee, D., Thépaut, J-N.: ERA5 hourly data on single levels from 1940 to present, Copernicus Climate Change Service (C3S) Climate Data Store (CDS), DOI: 10.24381/cds.adbb2d47, 2023.

Hofstra, N., Haylock, M., New, M., Jones, P., & Frei, C.: Comparison of six methods for the interpolation of daily, European climate data, Journal of Geophysical Research Atmospheres, 113(21). https://doi.org/10.1029/2008JD010100, 2008.

Hofstra, N., New, M.: Spatial variability in correlation decay distance and influence on angular-distance weighting interpolation of daily precipitation over Europe, International Journal of Climatology, 29*(12)*, 1872–1880, https://doi.org/10.1002/joc.1819 , 2009.

Hundecha, Y., Arheimer, B., Berg, P., Capell, R., Musuuza, J., Pechlivanidis, I., Photiadou, Ch.: Effect of model calibration strategy on climate projections of hydrological indicators at a continental scale, Climatic Change 163, 1287–1306, https://doi.org/10.1007/s10584-020-02874-4 , 2020.

Isotta, F.A., Frei, C., Weilguni, V., Percec Tadic, M., Lassegues, P., Rudolf, B., Vertacnik, G.: The climate of daily precipitation in the Alps: development and analysis of a high-resolution grid dataset from pan-Alpine rain-gauge data. Int. J. Climatol. 34 (5), 1657–1675, 2014.

Kottek, M., J. Grieser, C. Beck, B. Rudolf, F. Rubel: World Map of the Köppen-Geiger climate classification updated, Meteorol. Z., Vol. 15, No 3, 259-263, 2006.

Lemke, C.-D., Sperzel, T., Radke-Fretz, M., Schweim, C., Ziese, M., Gomes, G., Grimaldi, S. and Salamon, P.: The CEMS Meteorological Data Collection Centre Annual Report 2023, Publications Office of the European Union, Luxembourg, https://data.europa.eu/doi/10.2760/7720039, JRC140025, 2025.

Matthews, G., Baugh, C., Barnard, C., Carton De Wiart, C., Colonese, J., Decremer, D., Grimaldi, S., Hansford, E., Mazzetti, C., O'Regan, K., Pappenberger, F., Ramos, A., Salamon, P., Tasev, D., Prudhomme, C.: Chapter 14 - On the operational implementation of the European Flood Awareness System (EFAS), Editor(s): Thomas E. Adams, Chandana Gangodagamage, Thomas C. Pagano, Flood Forecasting (Second Edition), Academic Press, 251-298, ISBN 9780443140099, https://doi.org/10.1016/B978-0-443-14009-9.00005-5 , 2024.

Pedregosa, F., Varoquaux, G., Gramfort, A., Michel, V., Thirion, B., Grisel, O., Blondel, M., Prettenhofer, P., Weiss, R., Dubourg, V., Vanderplas, J., Passos, A., Cournapeau, D., Brucher, M., Perrot, M., Duchesnay, E.: Scikit-learn: Machine Learning in Python, Journal of Machine Learning Research, 2011.

Roberts, D. R., Bahn, V., Ciuti, S., Boyce, M. S., Elith, J., Guillera-Arroita, G., Hauenstein, S., Lahoz-Monfort, J. J., Schröder, B., Thuiller, W., Warton, D. I., Wintle, B. A., Hartig, F., & Dormann, C. F.: Cross-validation strategies for data with temporal, spatial, hierarchical, or phylogenetic structure, Ecography, Vol. 40, Issue 8, 913–929, Blackwell Publishing Ltd. https://doi.org/10.1111/ecog.02881, 2017.

Salamon, P., Sperzel, T., Gomes, G., Radke-Fretz, M., Lemke, C-D., Russo, C., Schweim, C., Zsoter, E., Dosio, A., Vomero, M., Ziese, M., Grimaldi, S.: EMO-1: an improved version of the high-resolution multi-variable gridded meteorological dataset for Europe. Joint Research Centre Data Catalogue, https://doi.org/10.2905/0BD84BE4-CEC8-4180-97A6-8B3ADAAC4D26 , 2025.

Schamm, K., Ziese, M., Becker, A., Finger, P., Meyer-Christoffer, A., Schneider, U., Schröder, M., & Stender, P.: Global gridded precipitation over land: A description of the new GPCC First Guess Daily product. Earth System Science Data, *6*(1), 49–60, https://doi.org/10.5194/essd-6-49-2014, 2014.

Shepard, D.: A two-dimensional interpolation for irregularly-spaced data function, Proc. 23rd ACM Nat. Conf, Ed. Brandon/Systems Press, 1968.

Spinoni, J., Szalai, S., Szentimrey, T., Lakatos, M., Bihari, Z., Nagy, A., Németh, Á., Kovács, T., Mihic, D., Dacic, M., Petrovic, P., Kržič, A., Hiebl, J., Auer, I., Milkovic, J., Štepánek, P., Zahradnícek, P., Kilar, P., Limanowka, D., Pyrc, R.,

Cheval, S., Birsan, M.-V., Dumitrescu, A., Deak, G., Matei, M., Antolovic, I., Nejedlík, P., Štastný, P., Kajaba, P., Bochnícek, O., Galo, D., Mikulová, K., Nabyvanets, Y., Skrynyk, O., Krakovska, S., Gnatiuk, N., Tolasz, R., Antofie, T. and Vogt, J.: Climate of the Carpathian Region in the period 1961–2010: climatologies and trends of 10 variables. Int. J. Climatol., 35, 1322-1341, https://doi.org/10.1002/joc.4059, 2015.

Thiemig, V., Gomes, G. N., Skøien, J. O., Ziese, M., Rauthe-Schöch, A., Rustemeier, E., Rehfeldt, K., Walawender, J. P., Kolbe, C., Pichon, D., Schweim, C., Salamon, P.: EMO-5: a high-resolution multi-variable gridded meteorological dataset for Europe, Earth Syst. Sci. Data, 14, 3249–3272, https://doi.org/10.5194/essd-14-3249-2022, 2022.

Tilloy, A., Paprotny, D., Grimaldi, S., Gomes, G., Bianchi, A., Lange, S., Beck, H., Mazzetti, C., and Feyen, L.: HERA: a high-resolution pan-European hydrological reanalysis (1951–2020), Earth Syst. Sci. Data, 17, 293–316, https://doi.org/10.5194/essd-17-293-2025, 2025.

Vautard, R., Kadygrov, N., Iles, C., Boberg, F., Buonomo, E., Bülow, K., Coppola, E., Corre, L., van Meijgaard, E., Nogherotto, R., Sandstad, M., Schwingshackl, C., Somot, S., Aalbers, E., Christensen, O.B., Ciarlo, J.M., Demory, M. E., Giorgi, F., Jacob, D., Jones, R.G., Keuler, K., Kjellström, E., Lenderink, G., Levavasseur, G., Nikulin, G., Sillmann, J., Solidoro, C., Sørland, S. L., Steger, C., Teichmann, C., Warrach-Sagi, K., Wulfmeyer, V.: Evaluation of the large EURO-CORDEX regional climate model ensemble. Journal of Geophysical Research: Atmospheres, 126, e2019JD032344. https://doi.org/10.1029/2019JD032344, 2021.

Willmott, C. J., Rowe, C. M., Philpot,W. D.: Small-scale cli- mate maps: A sensitivity analysis of some common assumptions associated with grid-point interpolation and contouring, Am. Cartographer, 12, 5–16, 1985.

World Meteorological Organization (WMO): Manual on Codes Volume I.1 Annex II to the WMO Technical Regulations Part A – Alphanumeric Codes, (WMO No.306, Part I.1 Part A), 2011 edition, updated in 2019, 480 pp., ISBN 978-92-63-10306-2, Geneva, Switzerland, 2019.

World Meteorological Organisation: State of Global Water Resources 2023, WMO-No. 1362, ISBN 978-92-63-11362-7, https://library.wmo.int/idurl/4/69033, 2024

Yamazaki, D., Ikeshima, D., Tawatari, R., Yamaguchi, T., O'Loughlin, F., Neal, J. C., Sampson, C. C., Kanae, S., Bates, P. D.: A high-accuracy map of global terrain elevations, Geophys. Res. Lett., 44, 5844–5853, https://doi.org/10.1002/2017GL072874, 2017.

https://doi.org/10.5194/essd-2025-723
Preprint. Discussion started: 4 March 2026

Yang, R., Xing, B : A comparison of the performance of different interpolation methods in replicating rainfall magnitudes under different climatic conditions in chongqing province (China). Atmosphere, 12*(10)*. https://doi.org/10.3390/atmos12101318, 2021.

605